

ornl

ORNL/TM-7068

**OAK
RIDGE
NATIONAL
LABORATORY**

**UNION
CARBIDE**

**Analysis of the Long-Term
Creep-Fatigue Behavior
of 2 $\frac{1}{4}$ Cr-1 Mo Steel**

M. K. Booker

This document has been reviewed and is determined to be
APPROVED FOR PUBLIC RELEASE.

Name/Title: Leesa Laymance/ORNL TIO

Date: 7/31/2020



**OPERATED BY
UNION CARBIDE CORPORATION
FOR THE UNITED STATES
DEPARTMENT OF ENERGY**

APPLIED TECHNOLOGY

Any further distribution by any holder of this document or of the data therein to third parties representing foreign interests, foreign governments, foreign companies, or foreign subsidiaries or foreign divisions of U.S. companies should be coordinated with the Director, Division of Reactor Research and Technology, Department of Energy.

Printed in the United States of America. Available from
the Department of Energy

Technical Information Center

P.O. Box 62, Oak Ridge, Tennessee 37830

Printed Copy A04 ; Microfiche A01

This report was prepared as an account of work sponsored by an agency of the United States Government. Neither the United States nor any agency thereof, nor any of their employees, makes any warranty, expressed or implied, or assumes any legal liability or responsibility for any third party's use or the results of such use of any information, apparatus, product or process disclosed in this report, or represents that its use by such third party would not infringe privately owned rights.

ORNL/TM-7068

Distribution


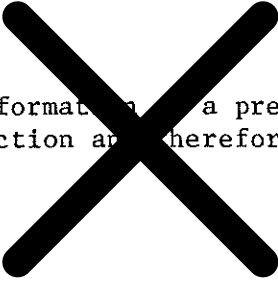
~~Categories UC 79a, k, r~~

Contract No. W-7405-eng-26

METALS AND CERAMICS DIVISION

ANALYSIS OF THE LONG-TERM CREEP-FATIGUE
BEHAVIOR OF 2 1/4 Cr-1 Mo Steel

M. K. Booker

 **Notice.** This document contains information of a preliminary nature.
It is subject to revision or correction and therefore does not represent
a final report. 

Date Published - December 1979

OAK RIDGE NATIONAL LABORATORY
Oak Ridge, Tennessee 37830
operated by
UNION CARBIDE CORPORATION
for the
DEPARTMENT OF ENERGY

CONTENTS

ABSTRACT	1
INTRODUCTION	1
LINEAR DAMAGE SUMMATION.	2
STRAIN RANGE PARTITIONING.	4
DAMAGE RATE APPROACH	12
CONTINUOUS CYCLINE FATIGUE	13
CREEP-RUPTURE BEHAVIOR	14
DAMAGE SUMMATION	16
PREDICTION OF LONG-TERM DATA	16
PREDICTIONS OF LONG-TERM BEHAVIOR.	19
RELAXATION CURVES.	20
LINEAR DAMAGE RESULTS.	20
STRAIN RANGE PARTITIONING RESULTS.	31
DAMAGE RATE RESULTS.	33
STATUS	33
CONCLUSIONS.	36
ACKNOWLEDGMENTS.	36
REFERENCES	37
APPENDIX	41

ANALYSIS OF THE LONG-TERM CREEP-FATIGUE BEHAVIOR OF
2 1/4 Cr-1 Mo STEEL*

M. K. Booker

ABSTRACT

Ferritic 2 1/4 Cr-1 Mo steel is one of four materials currently approved for use in elevated-temperature service in nuclear power generation systems by ASME Code Case N-47. The Code Case includes elastic analysis creep-fatigue design curves for the other three materials, but not for 2 1/4 Cr-1 Mo steel. This report details our development of such curves for this material at the request of the ASME Working Group on Creep-Fatigue.

We examined available creep-fatigue data by linear summation of creep and fatigue damage, strain range partitioning, and damage rate analysis to guide us in the development of elastic analysis curves. The data are most consistent with the strain range partitioning predictions, but linear summation is the only approach currently recognized by Code Case N-47 for treatment of creep-fatigue analyses. For this reason we primarily developed elastic analysis curves with the linear summation of damage approach. Our other results are presented for comparison only.

The linear summation elastic analysis curves are constructed for maximum temperatures of 427, 482, and 538°C (800, 900, and 1000°F) for times of 100, 1000, 10,000, 80,000, and 250,000 h. In addition we constructed 100 h curves for a maximum temperature of 593°C (1100°F). Curves are constructed by using both the damage summation diagram from analysis of experimental data and an assumed damage sum of unity. The damage diagram results are recommended for use. We include final recommended design curves (including Poisson's ratio correction for ASME Code strain calculation formulae) for potential creep at both ends of the fatigue cycle (no mean stress) and for creep on the compressive end of the cycle (tensile mean stress) only.

INTRODUCTION

The prediction of long-term material behavior under combined creep and fatigue loading is an important but difficult aspect of elevated-temperature design. Many methods for prediction have been proposed and

*Work performed under DOE/RRT 189a OH028, Steam Generator Materials Development.

used with varying degrees of success. A recent report¹ summarizes many current views on the treatment of creep-fatigue data.

In some cases detailed inelastic analysis of all components in a given design may not be necessary. For these instances ASME Code Case N-47² includes elastic analysis creep-fatigue curves. However, the Code Case does not include such curves for 2 1/4 Cr-1 Mo steel. We report our efforts to develop those curves. In accordance with current design practice,² we predicted creep-fatigue behavior by linear summation of damage. Similar curves were developed two years ago and have been described in a previous report.³ Those curves, for design lives of 2.5×10^5 h, were reviewed by the ASME Working Group on Creep-Fatigue; the Working Group recommended minor changes. However, they recently requested that elastic analysis for shorter design lives be developed as well. In the meantime we have developed improved expressions for continuous cycling fatigue and creep-rupture behavior. Thus, to develop a consistent set of elastic analysis curves and to assure that the best available information is used in constructing the curves, we have developed a complete new set of elastic analysis curves (including 2.5×10^5 h curves). Though these new curves utilize the revised fatigue and creep-rupture expressions, they are developed similarly to the previous curves.³ For comparison the available data have also been examined by strain range partitioning⁴ and damage rates⁵ to describe creep-fatigue behavior.

LINEAR DAMAGE SUMMATION

Linear damage summation is based on the two distinct and separate types of damage that can develop at high temperatures. Creep damage is measured by the well-known time-fraction⁶ approach, while fatigue damage is accounted for by cycle fractions.⁷ Thus, at failure the damage reaches some critical value, D , given by

$$D = D_c + D_f , \quad (1)$$

where the creep damage, D_c , is given by

$$D_c = \sum_i \frac{t}{t_{ri}} , \quad (2)$$

and the failure damage, D_F , is given by

$$D_F = \sum_j \frac{n}{N_{fj}} , \quad (3)$$

where t and n represent the time and the number of cycles, respectively, spent in a given loading condition, and t_r and N_f represent the corresponding creep rupture life and the continuous-cycling fatigue life, respectively, under each condition.

The application of this method to available creep-fatigue data for 2 1/4 Cr-1 Mo steel is based on the approach outlined by Campbell.⁸ This method involves numerical integration of a relaxation curve during a hold period to calculate the creep damage per cycle as

$$D_c(1) = \int_0^{t_h} dt/t_r , \quad (4)$$

where t_h is the total hold time. Evaluation of $D_c(1)$ for a typical cycle then approximately gives the total creep damage at failure by

$$D_c = N_h D_c(1) , \quad (5)$$

where N_h is the total number of cycles to failure in the given hold-time test. For available experimental creep-fatigue data, the strain range and temperature were always held constant so that the fatigue damage for a given test is given by

$$D_F = N_h/N_f . \quad (6)$$

Linear damage summation has been widely used, although it probably oversimplifies real behavior. Some of its obvious advantages are that it is:

1. based on widely available monotonic creep-rupture and continuous cycling fatigue data,
2. backed by considerable experience and recommended by Code Case N-47,
3. simple to apply and fits in with current stress analysis techniques and constitutive equations, and
4. relatively amenable to application of safety factors.

On the other hand, certain disadvantages are also evident:

1. monotonic tensile creep-rupture properties are used with cyclic loading, compression creep, etc.;
2. effects such as environmental interaction, metallurgical change such as thermal aging, and creep-fatigue interactions are not treated directly;
3. stresses are usually not known very accurately, and rupture life is very sensitive to stress;
4. D is very difficult to estimate if it is not unity, and it is somewhat difficult to determine if it is unity;
5. damage accumulation may not be linear with time but may vary with strain rate, etc.

STRAIN RANGE PARTITIONING

Our analysis of the creep-fatigue behavior of 2 1/4 Cr-1 Mo steel by strain range partitioning (SRP) has been described previously.⁹⁻¹⁰ Although not officially sanctioned by ASME Code Case N-47, this method has received considerable attention as a possible alternative approach, as witnessed by a recent symposium¹¹ devoted to discussion of experiences with the method.

The SRP procedure has been refined and modified during the last few years. The method used here is fairly basic. Briefly, the method assumes that the inelastic strain range traversed by a cycling specimen can be partitioned into four possible components:

$\Delta\epsilon_{pp}$ = tensile plastic strain reversed by compressive plastic strain,

$\Delta\epsilon_{cc}$ = tensile creep strain reversed by compressive creep strain,

$\Delta\epsilon_{cp}$ = tensile creep strain reversed by compressive plastic strain, and

$\Delta\epsilon_{pc}$ = tensile plastic strain reversed by compressive creep strain.

Here "plastic" strain is defined as time-independent inelastic strain, while "creep" strain is defined as time-dependent inelastic strain.

Under a given set of loading conditions, the predicted cyclic life is found from the so-called "Interaction Damage Rule"¹² by

$$\frac{1}{N_{pred}} = \frac{F_{pp}}{N_{pp}} + \frac{F_{pc}}{N_{pc}} + \frac{F_{cp}}{N_{cp}} + \frac{F_{cc}}{N_{cc}}, \quad (7)$$

where

N_{pred} = the predicted cyclic life,

$F_{pp} = \Delta\epsilon_{pp}/\Delta\epsilon_{in}$,

$F_{pc} = \Delta\epsilon_{pc}/\Delta\epsilon_{in}$,

$F_{cp} = \Delta\epsilon_{cp}/\Delta\epsilon_{in}$,

$F_{cc} = \Delta\epsilon_{cc}/\Delta\epsilon_{in}$.

The value $\Delta\epsilon_{in}$ is the total inelastic strain range, while the inelastic strain components are defined above.

The quantities N_{pp} , N_{pc} , N_{cp} , and N_{cc} are the partitioned lines and refer to the expected cyclic life as if all the inelastic strain had been that component ($\Delta\epsilon_{pp}$, $\Delta\epsilon_{pc}$, $\Delta\epsilon_{cp}$, $\Delta\epsilon_{cc}$). These lines are defined for 2 1/4 Cr-1 Mo Steel by the following "life relationships":

$$N_{cp} = 255\Delta\epsilon_{in}^{-1.77}, \quad (8)$$

$$N_{cc} = 450\Delta\epsilon_{in}^{-1.24}, \quad (9)$$

$$N_{pc} = 386 \Delta \epsilon_{in}^{-1.07} , \quad (10)$$

$$N_{pp} = 521 \Delta \epsilon_{in}^{-2.67} (\Delta \epsilon_{in} < 0.45\%) , \quad (11)$$

$$N_{pp} = 1648 \Delta \epsilon_{in}^{-1.24} (\Delta \epsilon_{in} > 0.45\%) , \quad (12)$$

where $\Delta \epsilon_{in}$ values are measured in percent. Note that in formulating the best fit life relationship lines expressed by Eqs. (8) through (12), we used all cyclic creep and relaxation data, even though the particular damage strain fraction¹³ for a given test, that is $\phi = (F_{cc})(N_{obs}/N_{cc}) > 0.5$ for a "cc" cycle, was not obeyed. In the strain controlled relaxation tests, particularly those conducted at low total strain ranges, $\Delta \epsilon_{pp}$ was always the most dominant inelastic strain range. However, we thought it appropriate to include the strain controlled data in these formulations since our purpose was to generate guideline relationships for the design conditions referred to in the Introduction.

Note that Eqs. (11) and (12) merely describe the relationship between cyclic life and plastic strain range from continuous cycling tests. These expressions differ somewhat from those developed recently¹⁴ to describe this relationship; that report also includes a detailed analysis of temperature, heat-to-heat, and heat-treatment effects. Equations (11) and (12) represent a less detailed analysis but yield good compromise estimates of behavior. Secondary effects such as those listed above are commonly ignored in the SRP analysis.¹⁵ Figures 1 and 2 show the life relationships and the data used to obtain them, while Fig. 3 compares the four life relationship lines on a common axis.

Figure 4 summarizes results obtained by "back-predicting" the cyclic lines of the available experimental tests. In general, the results are quite satisfactory. However, there are indications in both Fig. 2(c) and 4(c) that "cc" strain when obtained via relaxation is particularly damaging. In view of this observation we constructed separate life relationship lines for creep "cc" strain and relaxation "cc" strain [denoted "cc(r)"] (Fig. 5). Figure 6 shows the results of back-predicting the

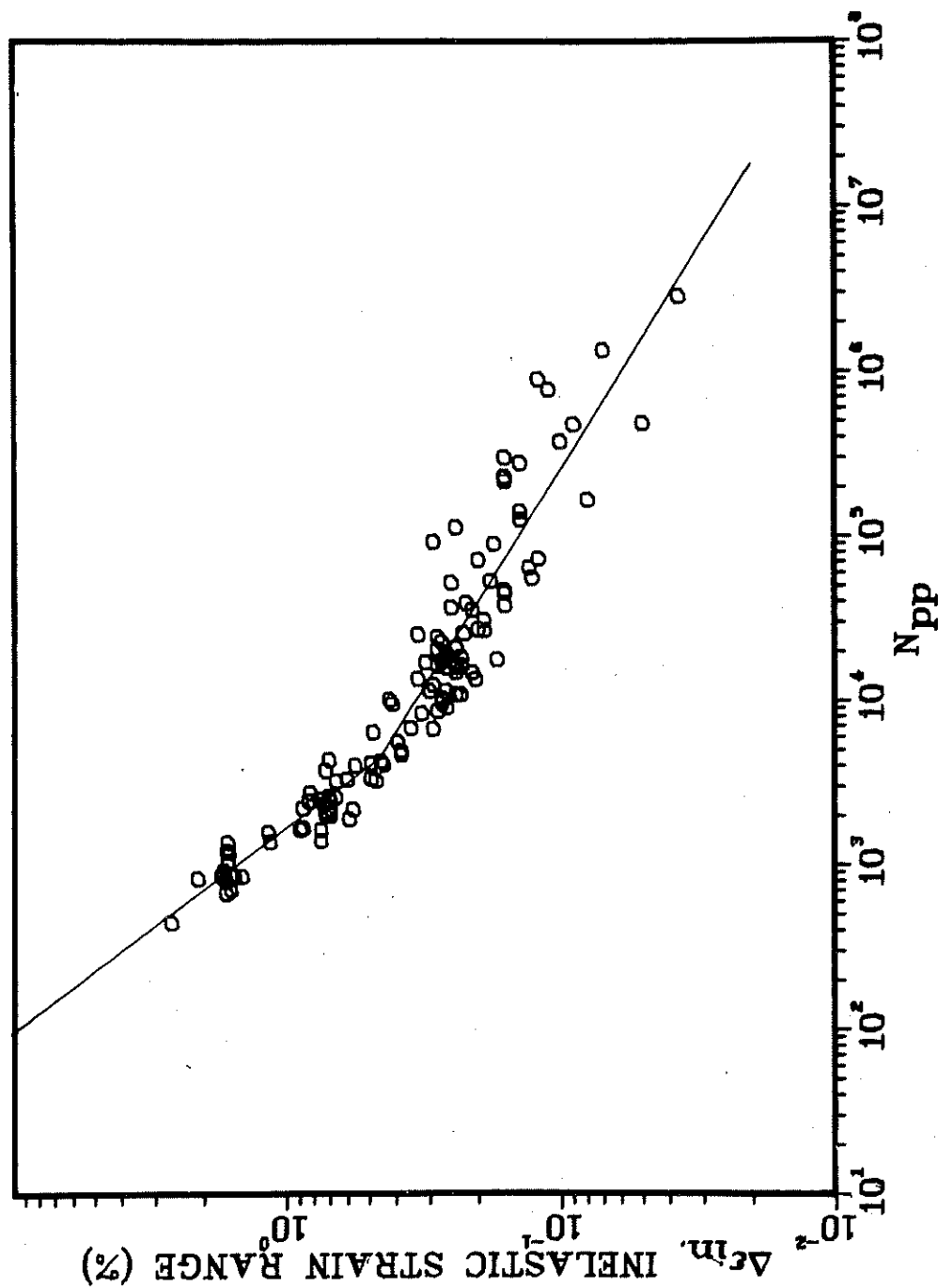
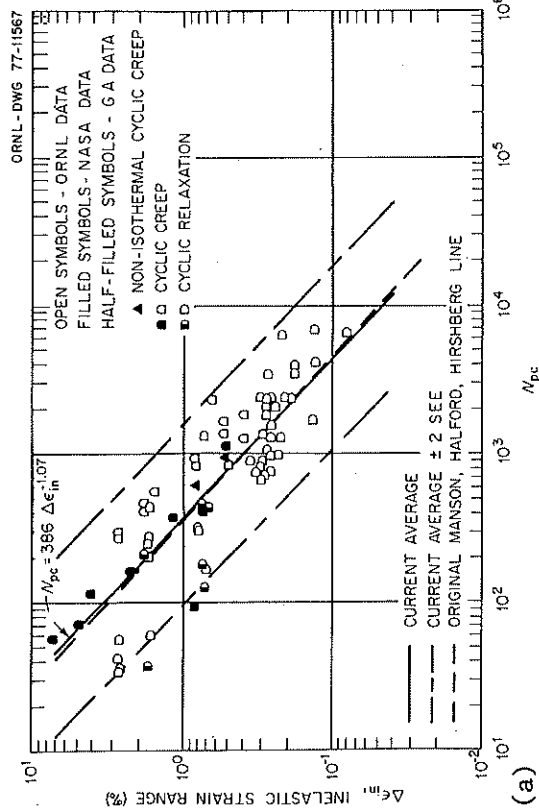
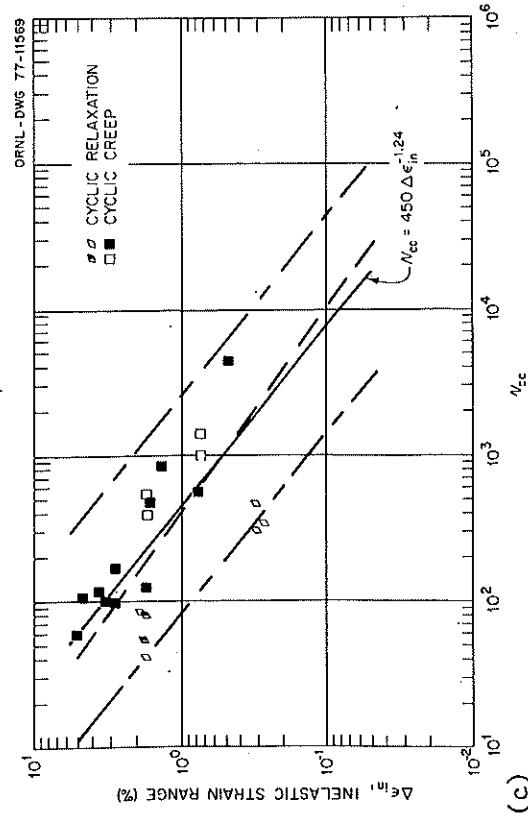


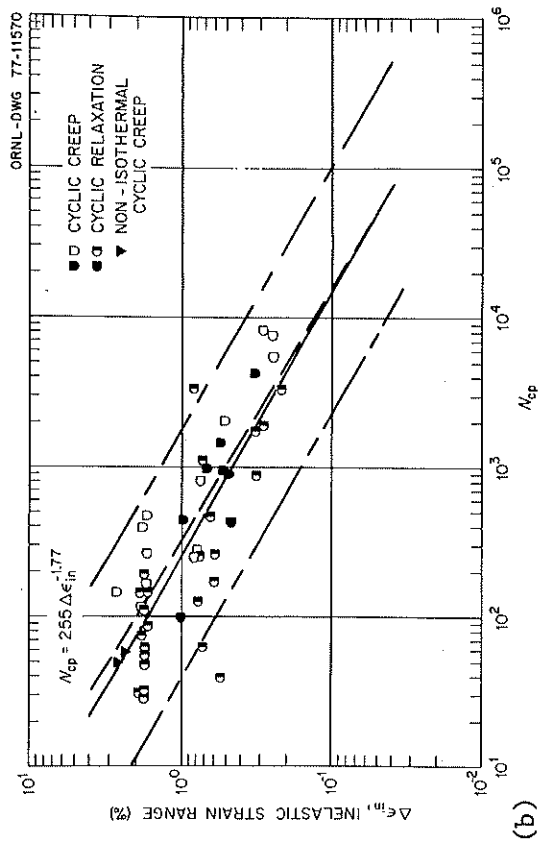
Fig. 1. Strain Range Partitioning Life Relationship Line for "pp" Strain for 2 1/4 Cr-1 Mo Steel.



(a)



(c)



(b)

Fig. 2. Strain Range Partitioning Life Relationship Lines for 2 1/4 Cr-1 Mo Steel:
 (a) "pc" Strain, (b) "cp" Strain, and (c) "cc" Strain.

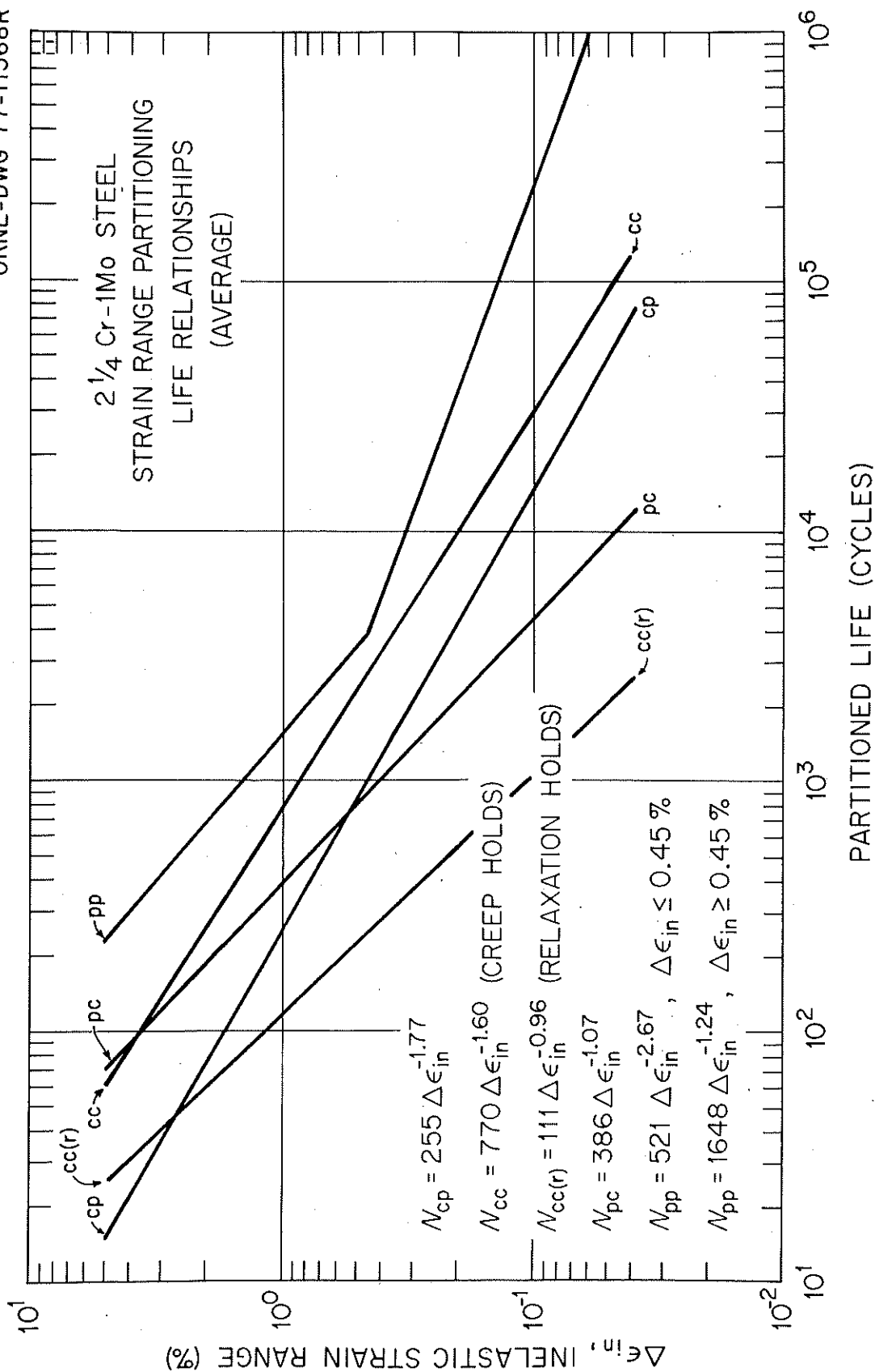
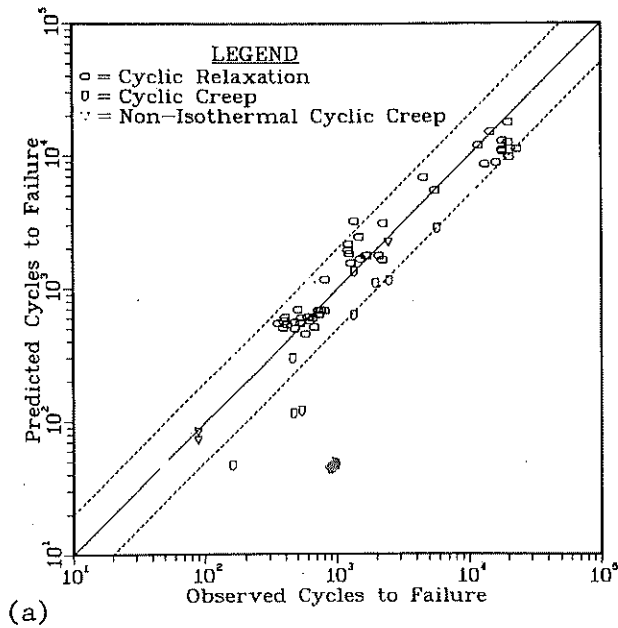


Fig. 3. Comparison of Various Strain Range Partitioning Life Relationship Lines for 2 1/4 Cr-1 Mo Steel.

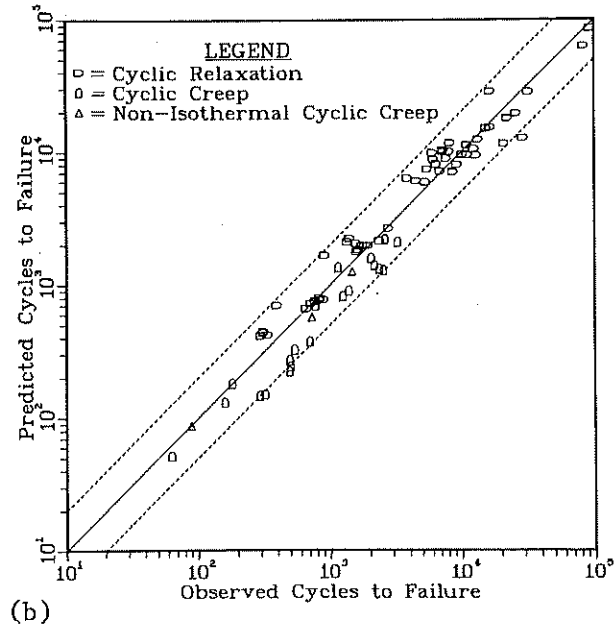
ORNL-DWG 77-12724

Tensile Holds



ORNL-DWG 77-12725

Compressive Holds



ORNL-DWG 77-12726

Tensile and Compressive Holds

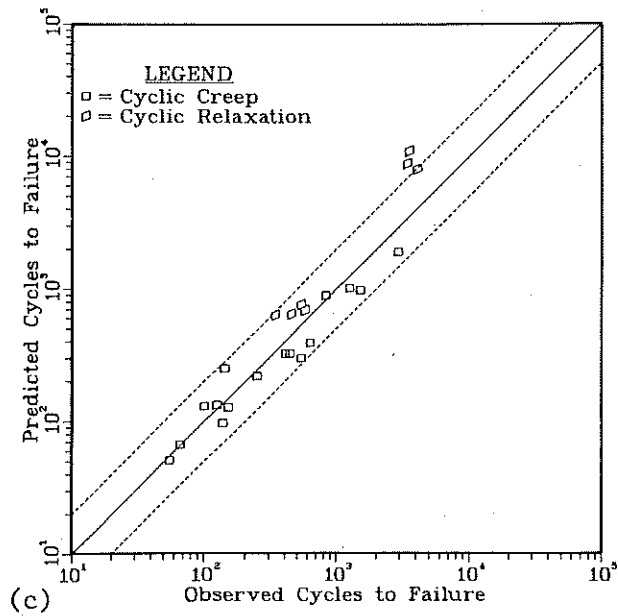


Fig. 4. Results of Back-Predicting Cyclic Lives of
 (a) Tensile Hold-Period (*cp*) Tests,
 (b) Compressive Hold-Period (*pc*) Tests, and (c) Tensile and Compressive Hold-Period (*cc*) Tests by Strain Range Partitioning.

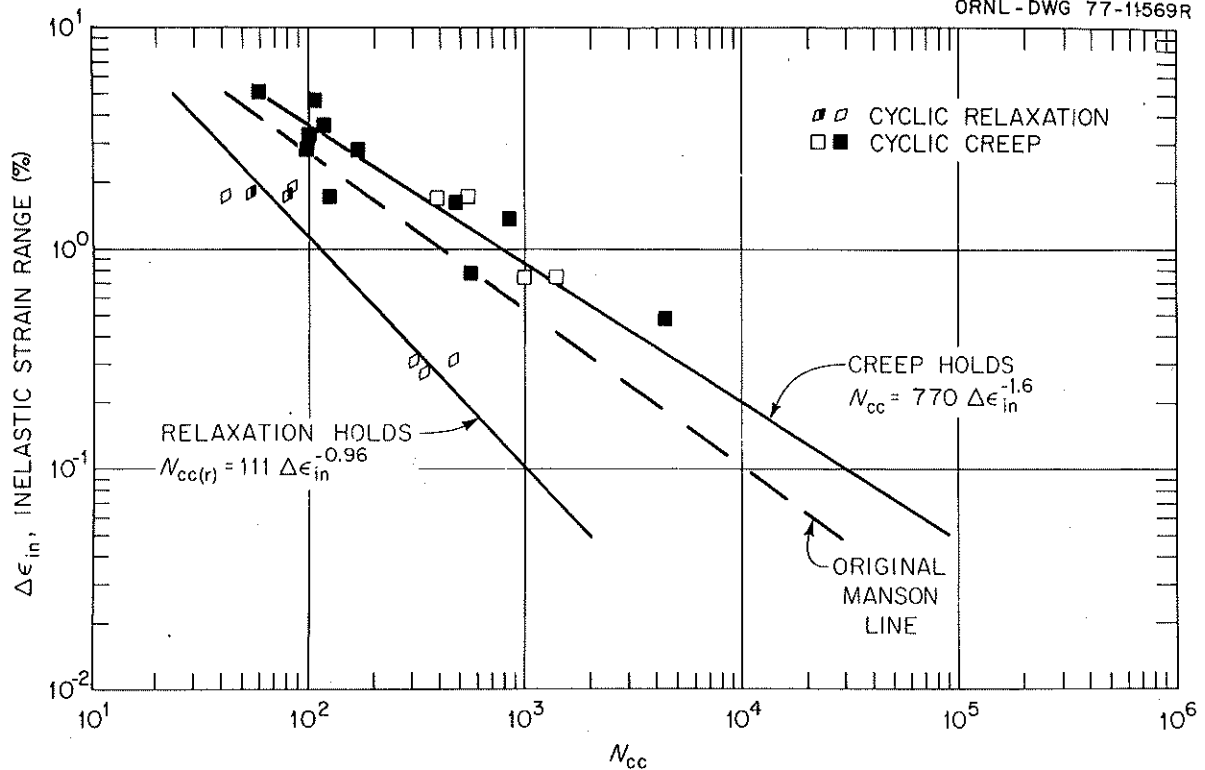


Fig. 5. Strain Range Partitioning Life Relationship Lines for 2 1/4 Cr-1 Mo Steel Treating " cc " Strain Resulting from Creep and " cc " Strain [" $cc(r)$ "] Resulting from Relaxation Separately.

ORNL-DWG 77-13787

Compressive Holds

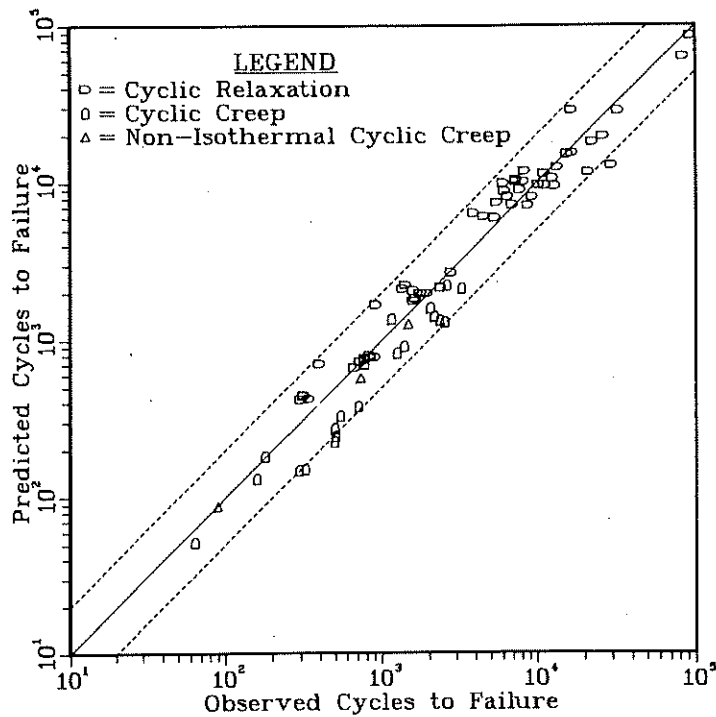


Fig. 6. Results of Back-Predicting Cyclic Lives of Tensile and Compressive Hold-Period (cc) Tests by Strain Range Partitioning with Dual " cc " Life Relationship Lines.

cyclic lives of the "cc" tests with the dual life relationship lines of Fig. 5. Finally, Fig. 7 compares the dual "cc" lines with the other life relationship lines.

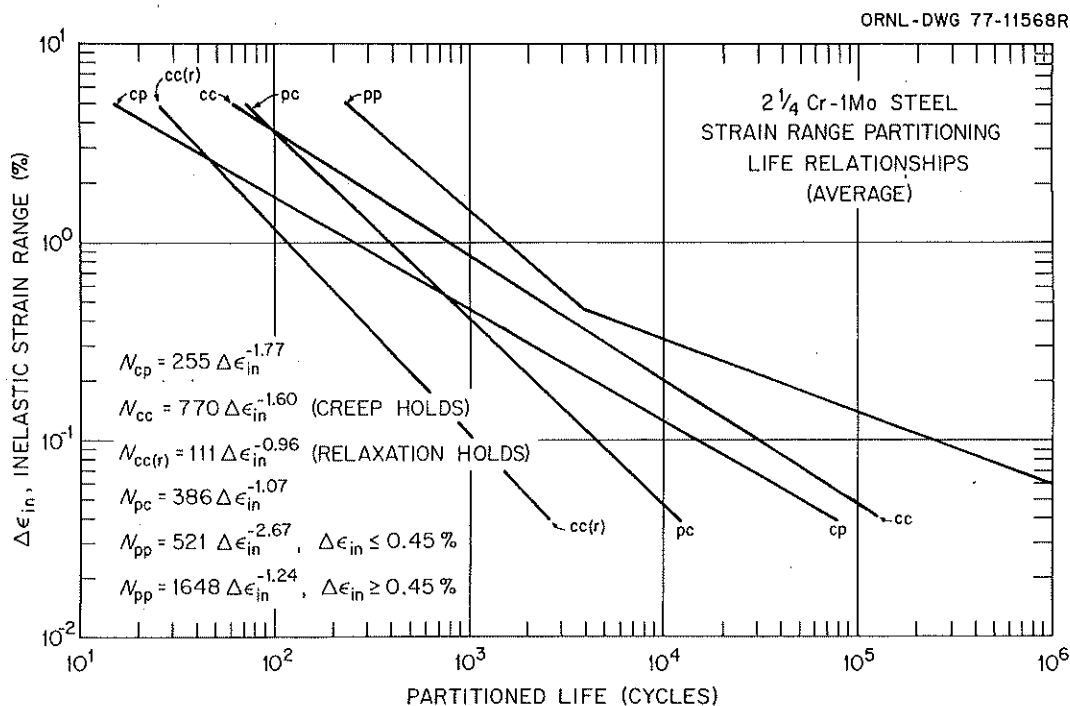


Fig. 7. Comparison of Dual "cc" Lines with Other Strain Range Partitioning Life Relationship Lines for 2 1/4 Cr-1 Mo Steel.

The implications of the above analysis in predicting long-term behavior must be assessed by comparison to actual data. For this reason we did not use several relatively long-term tests in construction of these life relationship lines. Comparison of predictions with these long-term data thus yields a true measure of the predictive capabilities of the method. This comparison will be discussed below.

DAMAGE RATE APPROACH

Another method for analytical description of creep-fatigue behavior that has received increasing attention is the "damage rate" approach of Majumdar et al.⁵ In that method both the amount of cyclic plastic strain

and the plastic strain rate at which the deformation occurs are important variables. Strains that accumulate more slowly are considered more damaging. The damage rate approach can be viewed as spreading the strain range partitioning discrete life relationships across a continuum of strain rates rather than merely separating them into slow (creep) and fast (plastic) rates.

We have not yet examined the damage rate approach for our data. However, Majumdar et al.⁵ examined a small set of data for 2 1/4 Cr-1 Mo steel and report preliminary results. To obtain a quick comparison of this method with the linear summation of damage and strain rate partitioning approaches, we simply extracted the equation constants from the Majumdar report, used the above relaxation curves from experimental tests, and predicted the cyclic lives for those tests using the damage rate life equations. Thus, our damage rate results should be considered more preliminary than the other predictions.

CONTINUOUS CYCLING FATIGUE

We calculated the continuous cycling fatigue life, N_f , to be used in the linear summation of damage calculations from a previous analysis.¹⁴ Briefly, that analysis separately relates plastic and elastic strain ranges to average cyclic life with the following equations:

Low Cycle

$$\Delta\epsilon_e = 0.736N_f^{-0.0959}, \quad (\leq 427^\circ\text{C}) \quad (13)$$

$$\Delta\epsilon_p = 252.9N_f^{-0.720}, \quad (14)$$

$$\Delta\epsilon_e = 0.606N_f^{-0.959}, \quad (538-593^\circ\text{C}) \quad (15)$$

$$\Delta\epsilon_p = 176.5N_f^{-0.720}; \quad (16)$$

High Cycle

$$\Delta \epsilon_e = 0.349 N_f^{-0.0287}, \quad (\leq 427^\circ\text{C}) \quad (17)$$

$$\Delta \epsilon_p = 11.62 N_f^{-0.370}, \quad (18)$$

$$\Delta \epsilon_e = 0.298 N_f^{-0.0287}, \quad (538-593^\circ\text{C}) \quad (19)$$

$$\Delta \epsilon_p = 9.71 N_f^{-0.370}. \quad (20)$$

In addition variable values of the coefficients in the above equations were calculated to allow a description of differences in behavior resulting from heat-to-heat or heat treatment effects on properties. Thus, in prediction of long-term behavior, the average equations above were used to estimate N_f . However, in the analysis of experimental data, N_f was estimated with the equations for the particular heat and heat treatment of concern.

CREEP-RUPTURE BEHAVIOR

Annealed 2 1/4 Cr-1 Mo steel can display significant differences in creep-rupture strength resulting from heat treatment and other effects. The rupture life, t_r (h), can be described by

$$\log t_r = -13.528 + 6.519U/T + \frac{23349}{T} - \frac{5693.8}{T} \log \sigma, \quad (21)$$

where all logarithms are base 10. Equation (1) was determined from a linear least squares fit to 121 data, yielding a coefficient of determination, R^2 , of 80.0% and a standard error of estimate, SEE, of 0.32. The stress, σ , is in MPa, and the temperature, T , is in K. The value in MPa of the ultimate tensile strength at the temperature of interest obtained at a strain rate of $6.7 \times 10^{-4}/\text{s}^1$ is U . The terms involving ultimate tensile strength allow the equation to reflect the above mentioned variations in strength level. Ideally, the value of U corresponds

to the particular heat and heat treatment of material under consideration. However, it may be appropriate to use an average value of U for material with the particular melting practice and heat treatment under consideration. Results are analytically valid under the following conditions:

$$\text{Stress} = 0 < |\sigma| < \text{ultimate tensile strength,}$$

$$\text{Temperature} = 427^{\circ}\text{C} (800^{\circ}\text{F}) \leq T \leq 593^{\circ}\text{C} (1100^{\circ}\text{F}).$$

The above equation was developed from data for air-melted, vacuum-arc remelted (VAR), and electroslog remelted (ESR) plate material. Heat treatments included both annealing and isothermal annealing with and without a subsequent 4-h postweld heat treatment at 727°C (1340°F). The predictions from the equation are quite consistent with the minimum stress to rupture values given for 2 1/4 Cr-1 Mo steel in Code Case N-47, as shown in Table 1.

Table 1. Comparison of Current Predictions with ASME Code Case N-47

Temperature		Ultimate Tensile Strength ^a (MPa)	Stress, MPa, for a Rupture Life, h, of ^b		
$^{\circ}\text{C}$	$(^{\circ}\text{F})$		10^1	10^3	10^5
454	(850)	450	450 ^c (-) ^d	320(-) ^d	178(185)
		345	345 ^c (358)	243(241)	135(145)
510	(950)	415	378(-) ^d	201(195)	107(108)
		310	287(276)	152(153)	81(87)
566	(1050)	345	226(228)	115(122)	58(61)
		240	172(179)	87(96)	44(48)

^aThe two values of ultimate tensile strength for each temperature represent approximate average and minimum values for annealed material (postweld heat-treated material can approach this minimum strength).

^bNonparenthesized values are from current predictions. Minimum values in parentheses are from ASME Code Case N-47. Average values in parentheses are from G. V. Smith, *Supplemental Report on the Elevated-Temperature Properties of Chromium-Molybdenum Steels (An Evaluation of 2 1/4 Cr-1 Mo Steel)*, ASTM DS 652, American Society for Testing and Materials, Philadelphia, Pa., 1971. Smith's work formed the basis of the values in Code Case N-47.

^cEquation predicts values greater than ultimate tensile strength. Value has been set as ultimate tensile strength.

^dConditions outside the range of predictions given in DS 652.

For estimation of long-term behavior by linear damage summation, average values of ultimate tensile strength for annealed air-melted 2 1/4 Cr-1 Mo steel¹⁶ were used in Eq. (21). In the analysis of experimental data, estimated tensile strength values for the particular heat and heat treatment were used to estimate rupture lives for use in the creep damage calculations.

DAMAGE SUMMATION

We calculated the linear summation of damage for available experimental data using the above continuous cycling fatigue and creep-rupture relationships. Note that both these relationships are different from those used previously³ in such calculations.

After the creep damage per cycle, $D_c(1)$, is calculated by Eq. (4) and N_f is estimated by Eqs. (13 through 20). The predicted cyclic life for a given test is then given by

$$N_h = \frac{D}{[1/N_f + D_c(1)]} \quad (22)$$

The value of D is often assumed to be 1. For the current data this assumption appeared reasonably good for tests involving tensile hold periods. However, for compressive hold periods (which are more damaging for this material at low strain ranges) a value of D less than 1 must be assumed to avoid overoptimistic predictions. As shown in Fig. 8, the bilinear "damage diagram" proposed in an earlier report³ still provides a good description of the available data. Therefore, this same diagram is again proposed for use here.

PREDICTION OF LONG-TERM DATA

Table 2 shows the relatively long-term creep-fatigue data for 2 1/4 Cr-1 Mo steel generated in the ORNL testing programs from 1977 through mid 1979. Also shown are predicted lives for those tests by strain range partitioning, linear summation of damage (using $D = 1$ and using the damage diagram), and damage rates. In general the damage diagram results agree

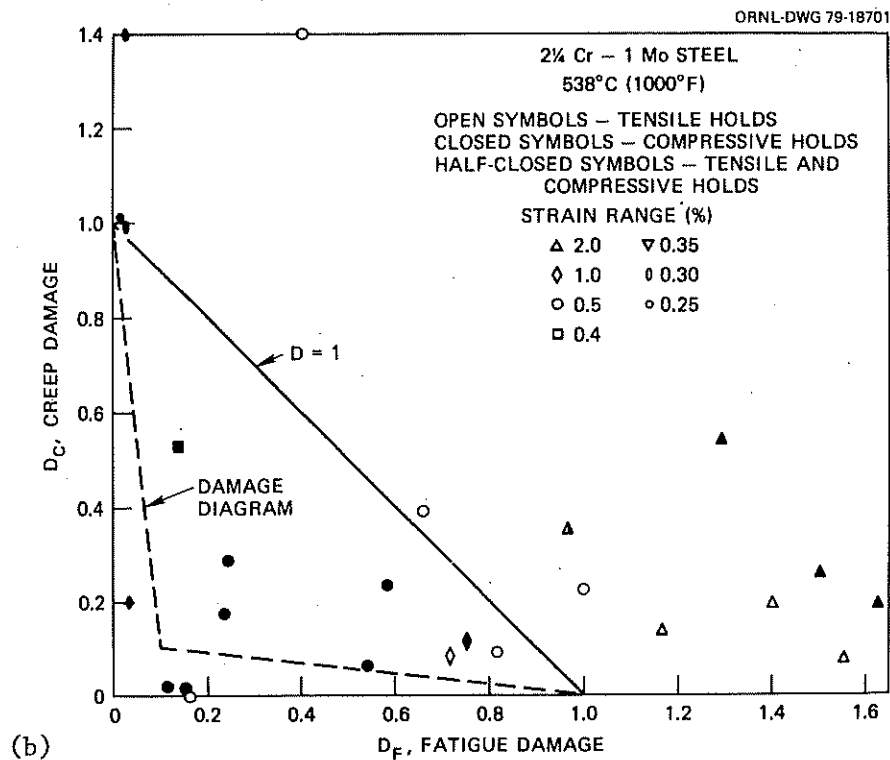
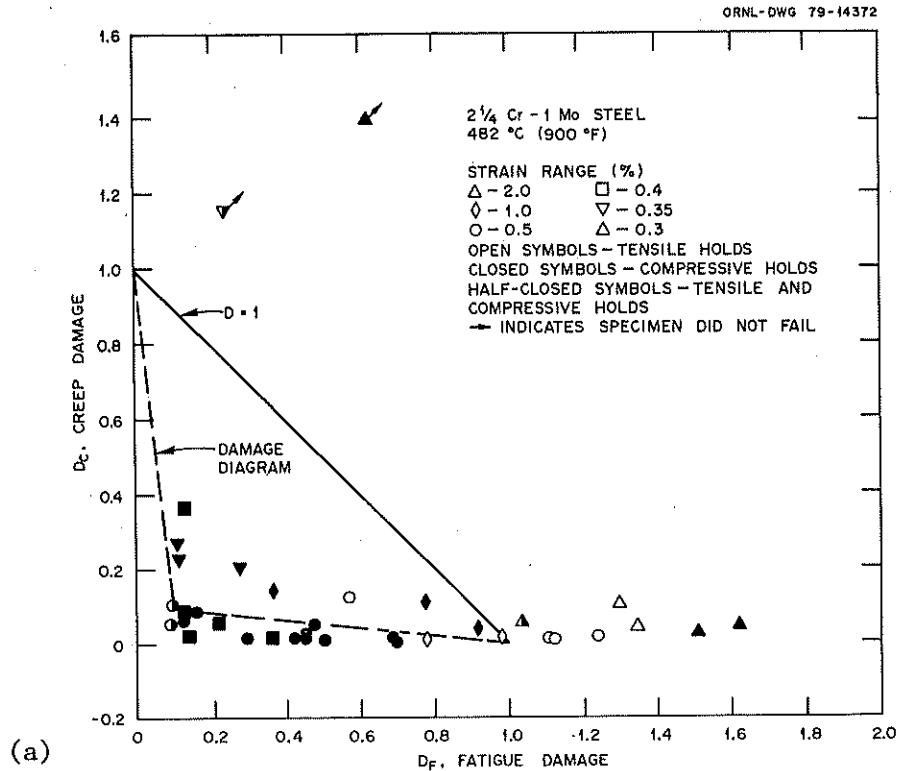


Fig. 8. Calculated Creep and Fatigue Damage for Creep-Fatigue Tests at (a) 482°C (900°F) and (b) 538°C (1000°F).

Table 2. Summary of Long-Term Creep-Fatigue Data for 2 1/4 Cr-1 Mo Steel

Specimen ^a	Temperature (°C)	Total Strain Range (%)	Hold Period ^b (h)	Cycles to Failure ^c	Time (Months)	Predicted Life Based on Strain-Range Partitioning	Predicted Life from Linear Damage Summation ($D = 1$)	Predicted Life from Linear Damage Summation Damage Diagram	Predicted Life from Damage Rate with Majumdar Constants ^d
MIL-65	482	0.5	0.1TC	3,420	1.0	8,794 (3775) ^e	16,803	3,472	4,390
ITT-30	482	0.48	0.05TC	3,525	0.5	7,218 (3320)	22,401	5,765	5,534
MIL-72	482	0.35	0.5TC	>71,000	9.9	34,541 (8036)	50,772	21,552	12,860
MIL-54	482	0.35	0.5C	34,995	2.4	41,181	101,753	27,405	18,240
MIL-61	482	0.30	0.01C	>600,000	8.6	442,168	222,888	78,034	62,450
MIL-60	482	0.35	0.1C	31,694	4.4	36,282	84,000	25,927	16,460
MIL-63	482	0.4	0.25C	14,936	5.0	12,030	30,572	10,060	10,710
MIL-69	538	0.3	0.05C	24,732	1.7	26,995	24,238	20,171	20,070
MIL-71	538	0.5	0.1T	14,023	1.9	8,736	7,376	2,746	6,649
MIT-3	538	0.3	0.1C	19,438	2.7	22,553	9,256	8,593	18,080
BIL-35	538	0.5	0.1(0)	5,680	0.7	8,627	35,000	35,000	7,930
VPH-24	482	0.5	0.25C	6,218	2.2	9,710	9,111	1,962	5,122
BIL-26	538	0.10	0.05C	>161,359 ^f	>11.3 ^f	349,000	5,900,000	5,900,000	192,000

^aAll specimens from annealed air-melted heat 3P5601 except VPH-24 from VAR heat 56447 with anneal + 40-h PWHT.^bC = compression; T = tension; (0) = hold at zero stress.^c> indicates test discontinued before failure.^dSource: S. Majumdar and P. S. Maiya, "A Damage Equation for Creep-Fatigue Interaction," pp. 323-35 in *Creep-Fatigue Interaction*, MPC-3, American Society of Mechanical Engineers, New York, 1976.^eValues in parentheses calculated with $ca(n)$ life relationship.^fTest presently ongoing.

better with the experimental compressive and compressive and tensile hold data than do the $D = 1$ results (as expected). Also, the SRP results generally describe the data better than do the linear damage results. The damage rate predictions tend to be very over conservative for the lowest strain range tests, probably as a result of the preliminary constants used in making those predictions. In particular, $\log \Delta \epsilon_p$ is assumed to be linearly related to $\log N_f$ at all strain levels, contrary to previous results.¹⁴ Note that all hold periods involved relaxation at peak strain rather than creep at peak stress. Still for specimen MIL-72 the combined "cc" life relationship line of Eq. (9) describes the data better than the "cc(r)" life relationship.

The low-strain-range tests in Table 2 generally tend to display longer cyclic lives than would be predicted by any of the techniques used. Moreover, the test on specimen BIL-35 indicates significant damaging effects resulting from a hold period at essentially zero strain, which none of the techniques predict.* Clearly, the creep-fatigue behavior of 2 1/4 Cr-1 Mo steel is a complex process. Recent progress,¹⁷ has been made toward development of detailed models for the process of time-dependent fatigue in this material. Our own current conclusion is that the process is strongly related to environmental effects. At any rate all of the techniques used here represent somewhat oversimplified views of the true material behavior, and one should keep this in mind in attempting to assess uncertainties in the long-term predictions.

PREDICTIONS OF LONG-TERM BEHAVIOR

To predict behavior for hold periods and time durations longer than those available experimentally, the linear damage summation approach requires that one be able to estimate long-term cyclic relaxation curves. This was done by first estimating the peak stress for the hold period³ and then estimating the actual relaxation curves from a creep equation.^{3,18,19}

*Both the strain range partitioning and damage rate approach well predict the life of this specimen, but only because they both under predict the continuous cycling life of this heat at these loading conditions.

The above expressions for rupture life and continuous-cycling fatigue life then allowed estimation of cyclic life under various hold-time conditions. These predictions were then used to construct elastic analysis curves. The peak stresses and total amount of predicted relaxation can also be used to estimate strain range components for use in long-term projections by strain range partitioning.

RELAXATION CURVES

The peak stresses used in estimating relaxation curves were the same as those used previously. Relaxation curves were also predicted, as was done previously. Details concerning calculation of the relaxation curves and estimation of creep and fatigue damage based on these curves are given in a former report.³

LINEAR DAMAGE RESULTS

We projected long-term creep-fatigue using the linear damage approach based on the above damage diagram for compressive holds and on the assumption that $D = 1$. Although we assumed that the peak stresses were constant throughout the life and that no creep strain hardening was carried over from one cycle to the next, the characteristics of the creep equation used to estimate relaxation behavior dictated that, in general, two types of relaxation curves were predicted within a given loading condition. For the first N_1 cycles, all predicted relaxation curves were of the first type; for the remaining $N_h - N_1$ cycles (N_h = predicted cycles to failure with hold time) the predicted relaxation curves were of the second type as a result of a metallurgical change in the material. Thus, the creep damage, D_c , is actually evaluated as:

$$D_c = N_1 \int_1^1 \frac{dt}{t_r} + (N_h - N_1) \int_1^2 \frac{dt}{t_r}, \quad (23)$$

or

$$D_c = N_1 D_c(1)_1 + (N_h - N_1) D_c(1)_2. \quad (24)$$

As a result Eq. (22) becomes

$$N_h = \frac{D - N_1[D_c(1)_1 - D_c(1)_2]}{[D_c(1)_2 + (1/N_f)]} \quad (25)$$

For the predictions using the damage diagram, the value of D is calculated by

$$D = \frac{N_1[D_c(1)_1 - D_c(1)_2](1 + B) - A[D_c(1)_2 N_f + 1]}{[B - D_c(1)_2 * N_f]}, \quad (26)$$

where $A = 1/9$ and $B = -1/9$ or $A = 1$ and $B = -9$, depending on which leg of the damage diagram the results fall on.

Typical projected results for given hold periods are shown in Figs. 9 and 10. However, note that these figures represent projections of average behavior. To estimate design behavior safety factors must be applied to the results. These factors were applied by design values of continuous cycling fatigue life¹⁴ in the above equations and by multiplying all creep damage quantities in the equations by 20; a factor of 20 on life is typically sought in ASME calculations of the creep portion of creep-fatigue damage.

Figures 11 and 12 illustrate typical predicted lives (with safety factors) for given hold periods. These projections can then be transformed into constant life design curves merely by taking appropriate time cuts across the curves in these figures. If the total design life is t_D , then the number of cycles to failure for a hold time of t_h is approximately given by t_D/t_h . Thus, for example, the allowable strain for a 10^4 cycle life in 10^4 h is the strain that would give a life of 10^4 h with a 1-h hold period in Figs. 11 and 12. By using this premise constant life curves were graphically constructed from results such as those in these two figures. Interpolation between the strain ranges shown was done on a linear log-log basis.

Figures 13 and 14 show various constant life curves constructed with the above technique. These curves are essentially the elastic analysis curves as currently defined by Code Case N-47. However, the Code method

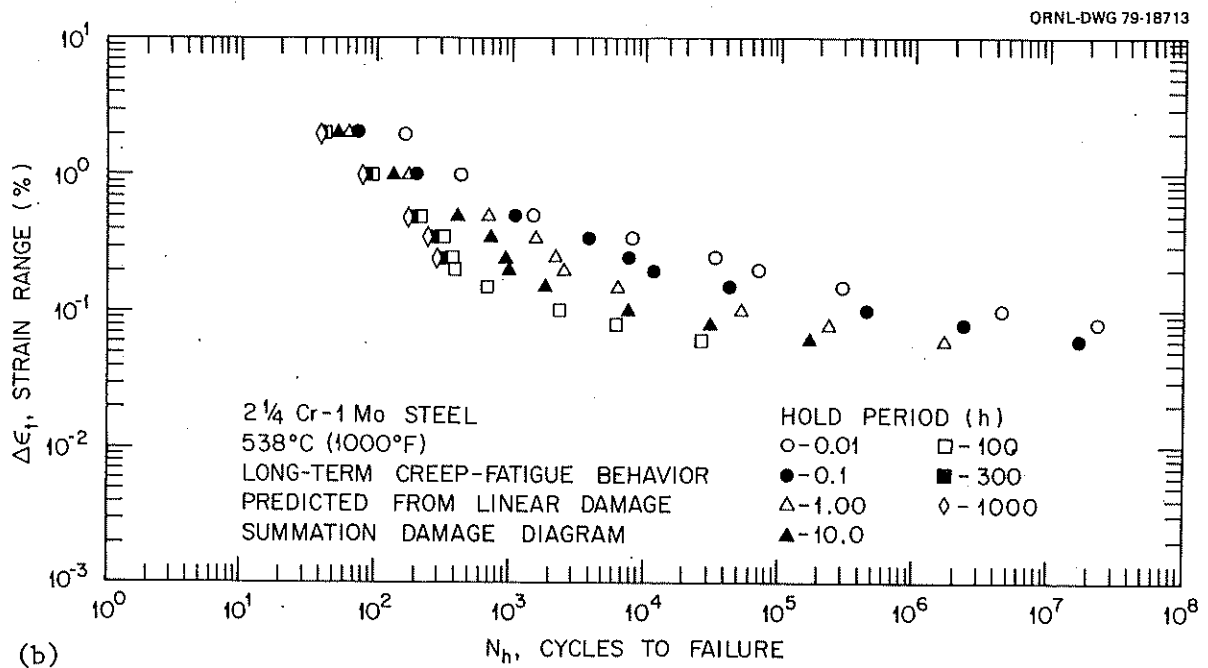
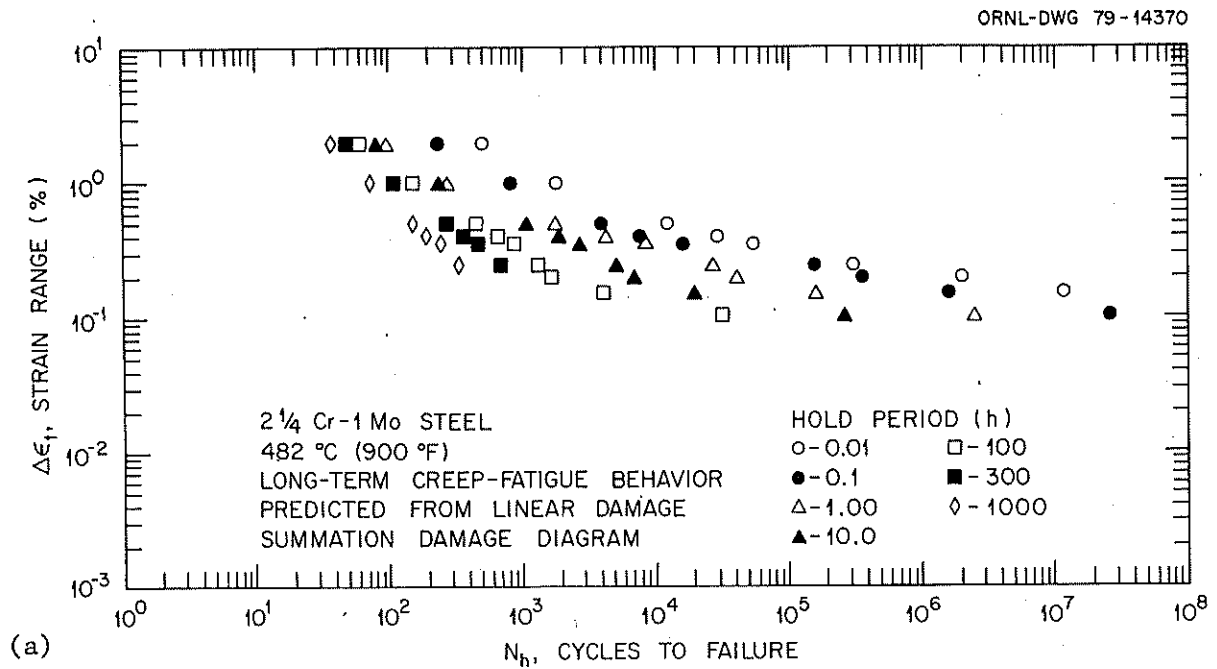


Fig. 9. Projected Average Creep-Fatigue Behavior by Linear Damage Summation with the Damage Diagram at (a) 482°C (900°F) and (b) 538°C (1000°F).

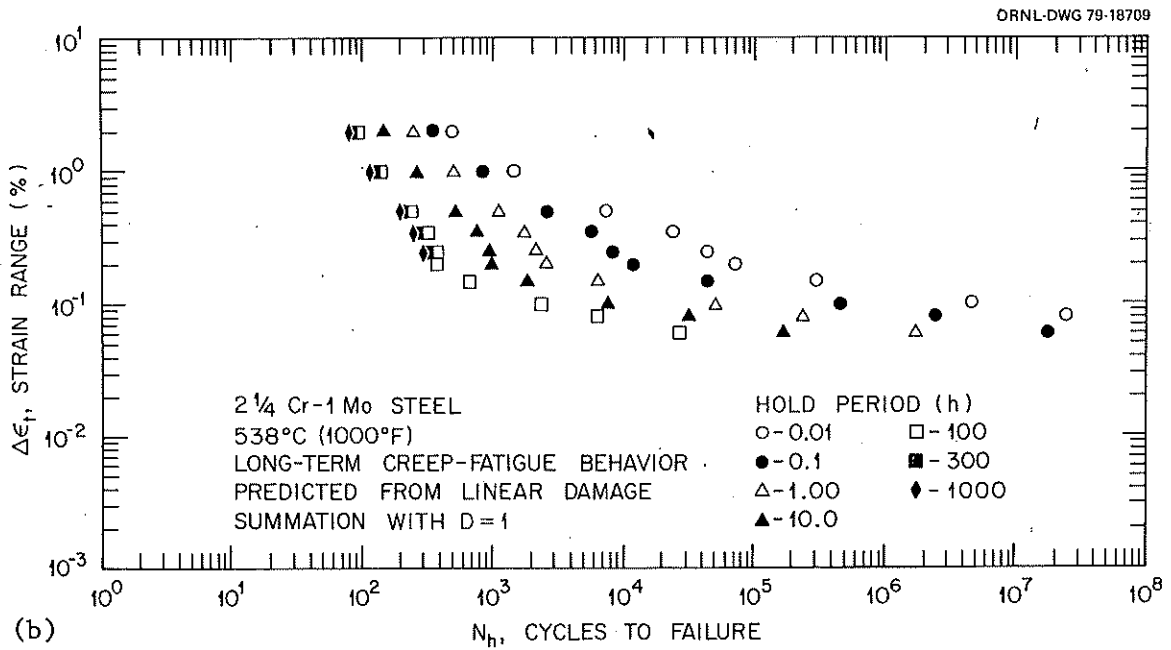
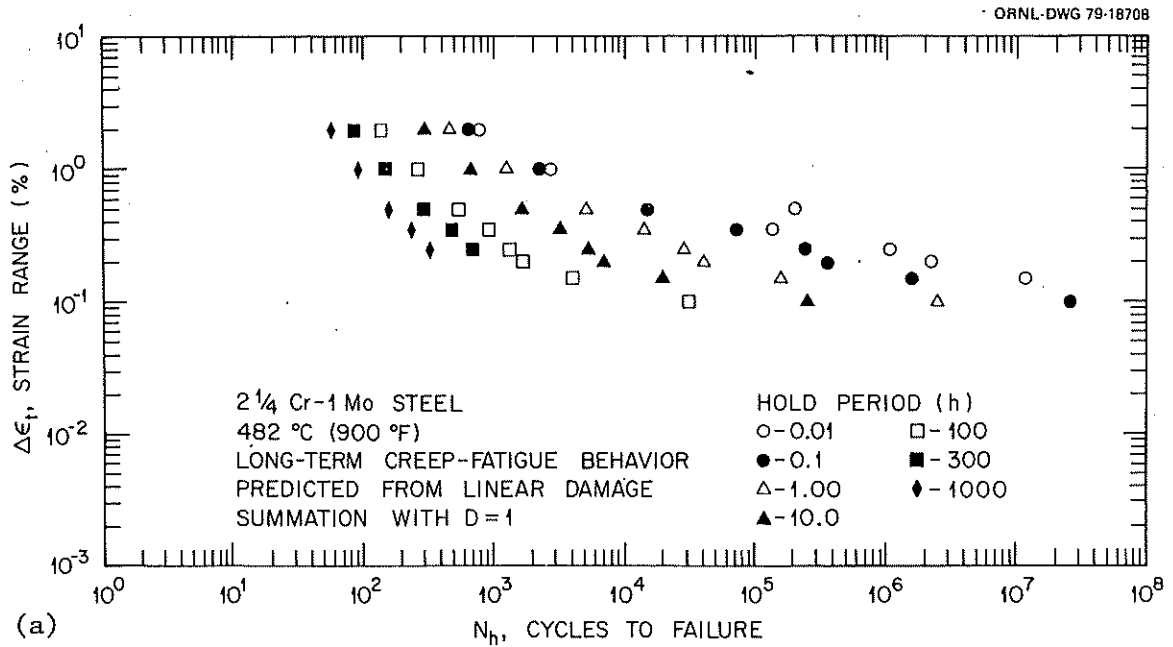


Fig. 10. Projected Average Creep-Fatigue Behavior by Linear Damage Summation with $D = 1$ at (a) 482°C (900°F) and (b) 538°C (1000°F).

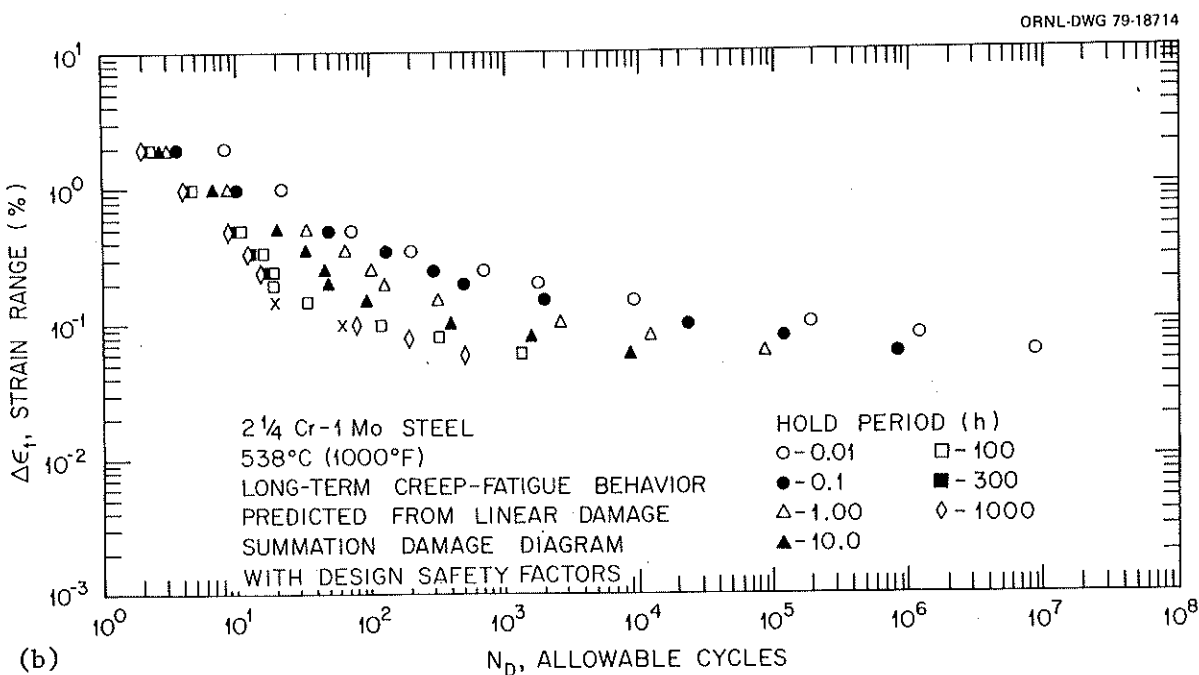
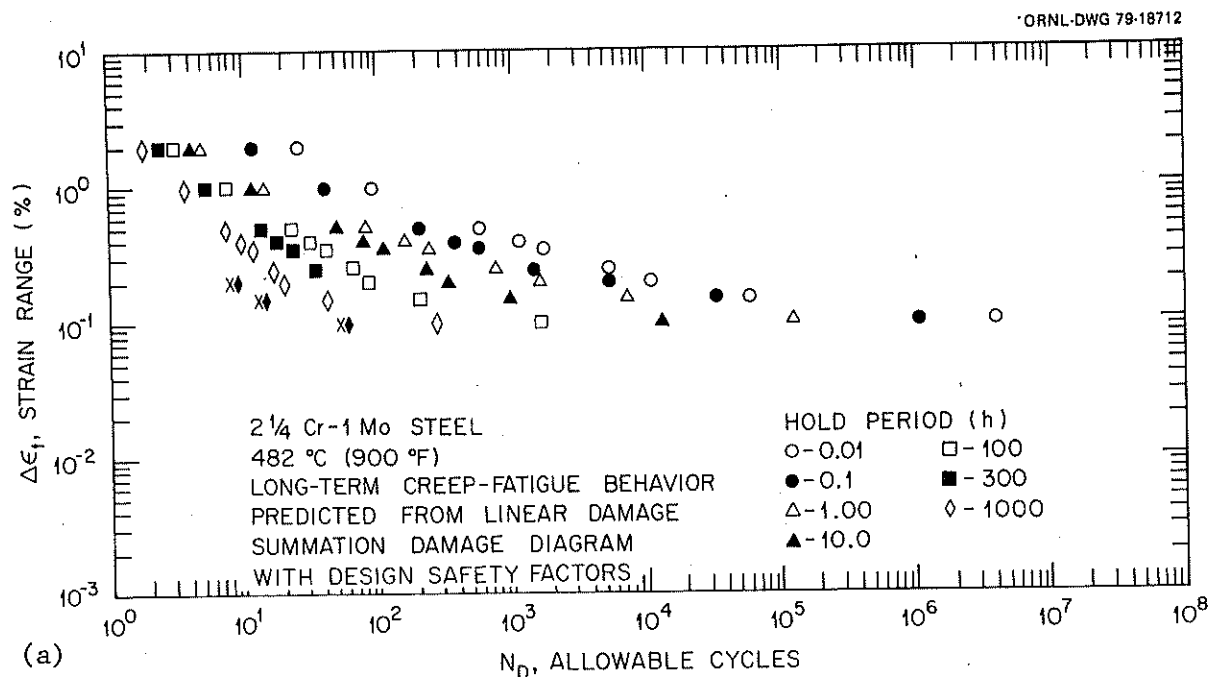


Fig. 11. Projected Creep-Fatigue Behavior with Design Safety Factors by Linear Damage Summation with the Damage Diagram at (a) 482°C (900°F) and (b) 538°C (1000°F).

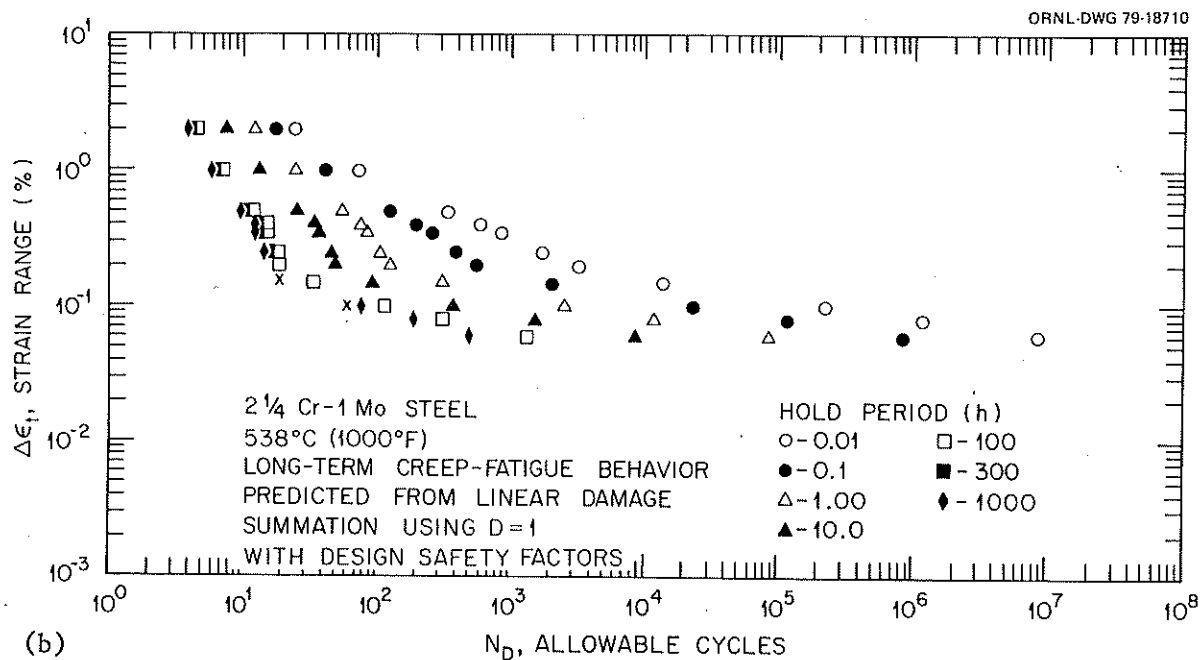
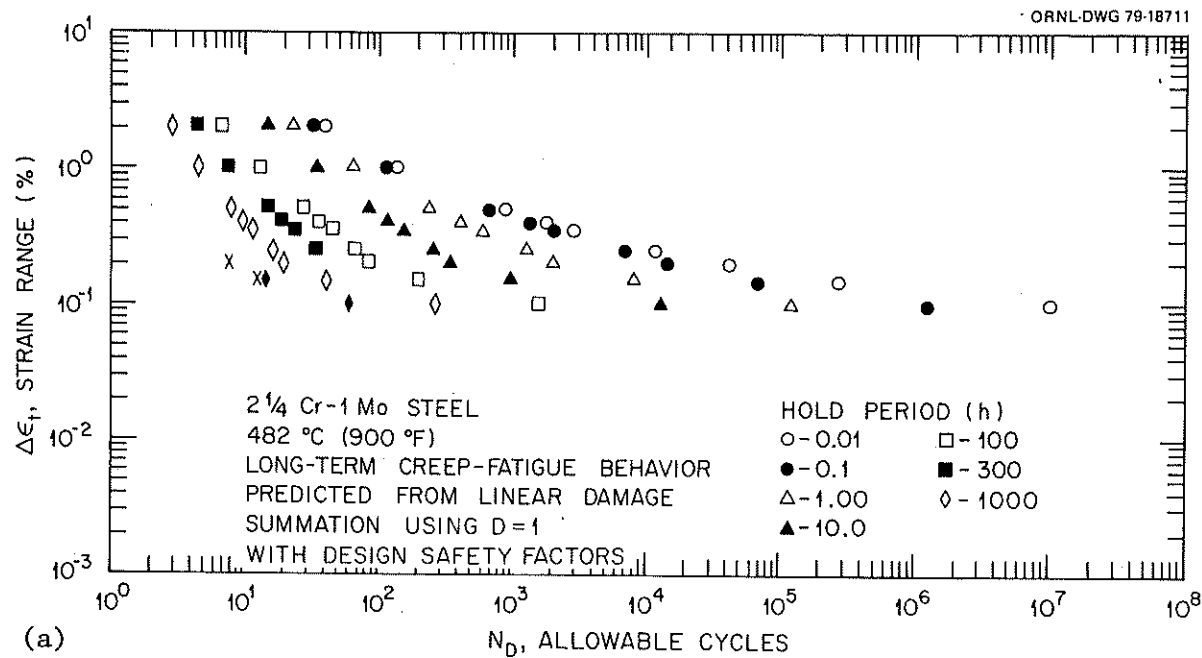
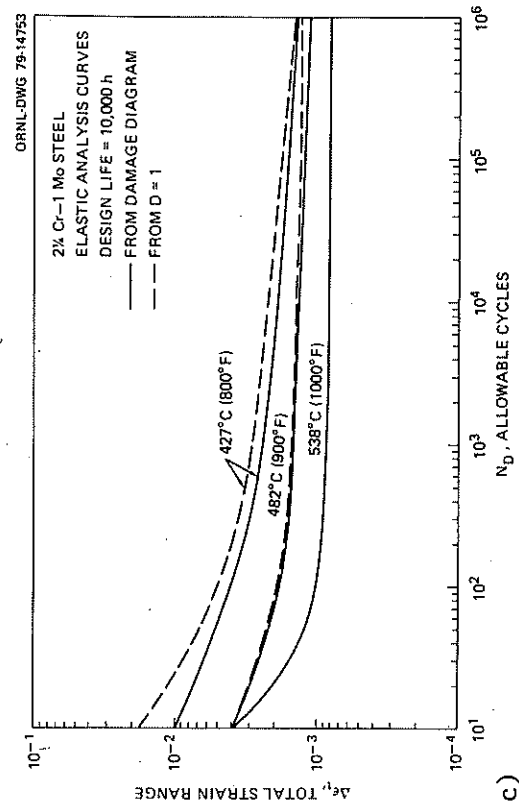
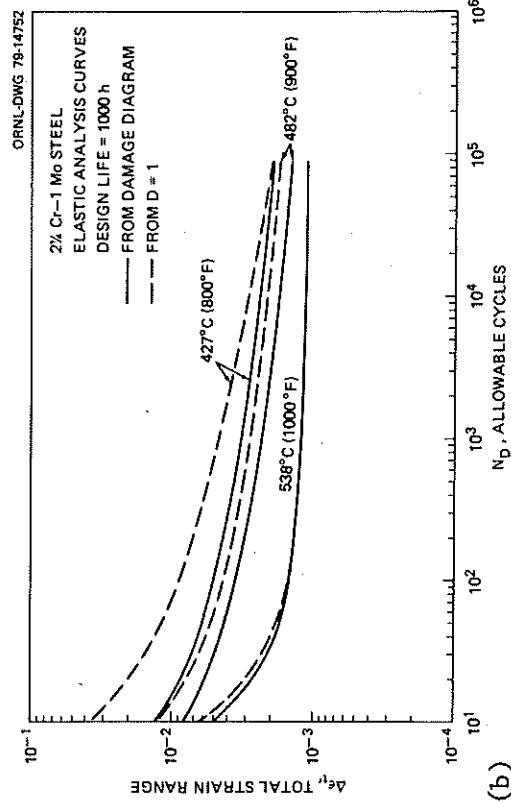
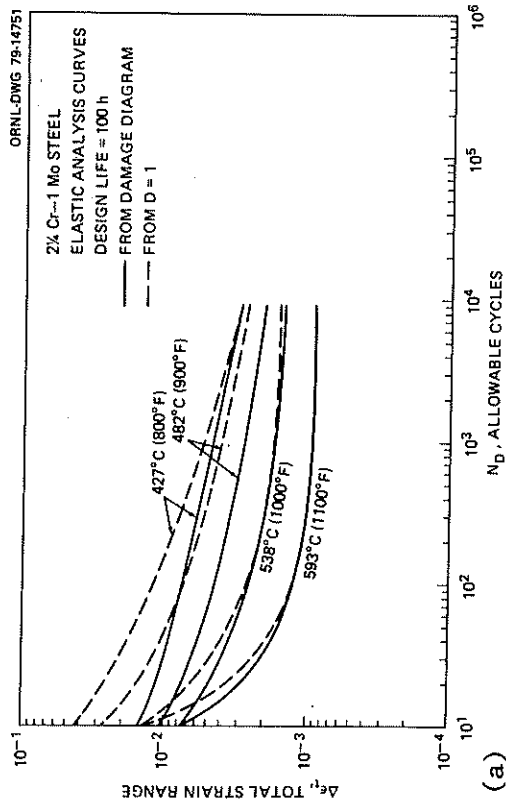
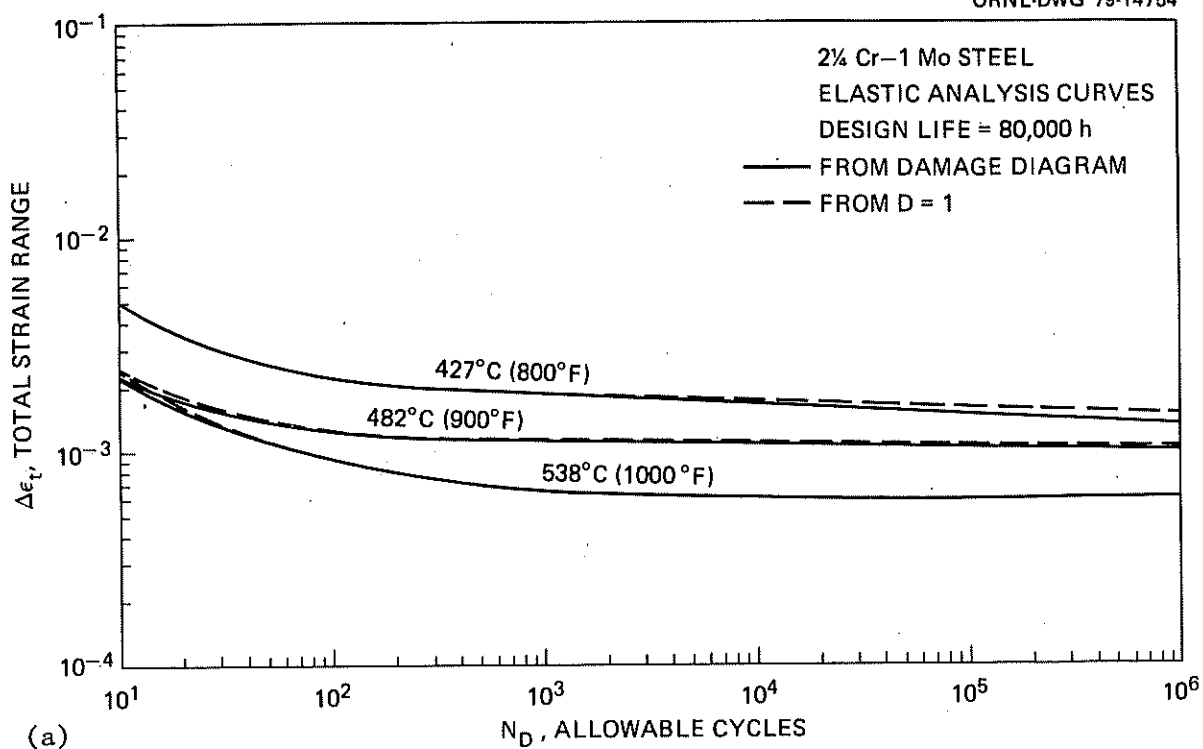


Fig. 12. Projected Creep-Fatigue Behavior with Design Safety Factors by Linear Damage Summation with $D = 1$ at (a) 482°C (900°F) and (b) 538°C (1000°F).

Fig. 13. Creep-Fatigue Curves with Design Safety Factors Calculated by Linear Damage Summation. Life = (a) 100, (b) 1000, and (c) 10,000 h.



ORNL-DWG 79-14754



ORNL-DWG 79-14371

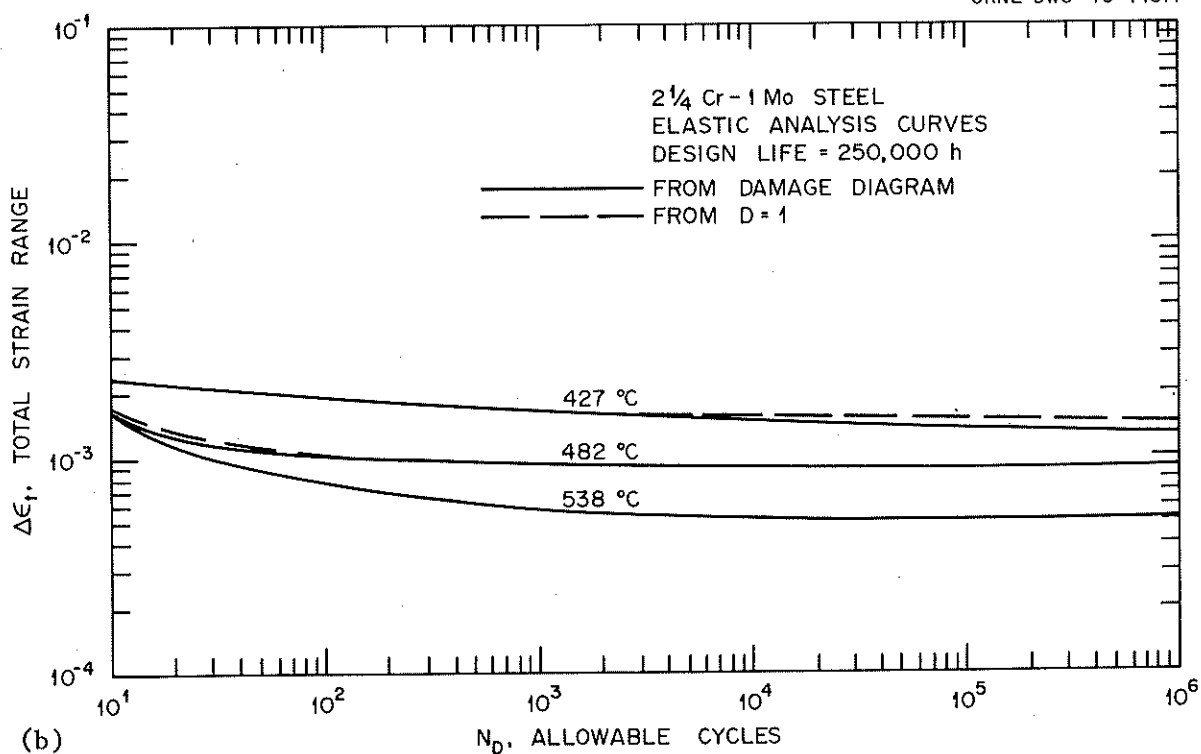


Fig. 14. Creep-Fatigue Curves with Design Safety Factors Calculated by Linear Damage Summation. Life = (a) 80,000 and (b) 250,000 h.

for estimating strain range uses an equivalent strain approach given by

$$\Delta\epsilon_{equiv} = \sqrt{\frac{2}{3}} [(\Delta\epsilon_x - \Delta\epsilon_y)^2 + (\Delta\epsilon_y - \Delta\epsilon_z)^2 + (\Delta\epsilon_z - \Delta\epsilon_x)^2 + \frac{3}{2} (\Delta\gamma_{xy}^2 + \Delta\gamma_{yz}^2 + \Delta\gamma_{zx}^2)]^{1/2} . \quad (27)$$

This equation is strictly applicable only to the case of purely plastic strain. For general cases the multiplier $\sqrt{2/3}$ should be replaced by $\sqrt{2/[2(1+\nu)]}$, where ν is Poisson's ratio. For plasticity $\nu = 0.5$, and the two approaches are identical. For purely elastic strain ν is of the order of 0.3, and the Code approach will underestimate the strain range by about 15%. Therefore, to avoid errors in prediction of fatigue damage, the curves in Figs. 13 and 14 were lowered by 15% in the high cycle and at 10^6 cycles to failure where the deformation is essentially elastic. (For short-time curves, the highest number of cycles shown was used for this calculation.) If $\Delta\epsilon^*$ is the strain range at 10^6 cycles in Figs. 13 and 14, this strain range decrement is given by $0.15\Delta\epsilon^*$. The remainder of the strain ranges was then decreased by this same amount, yielding curves that are essentially identical to those in Figs. 13 and 14 on the low cycle and where the deformation is essentially plastic. The final corrected design curves based on the damage diagram are given in Figs. 15 and 16.

Several characteristics of the curves in Figs. 13 and 14 should be noted. First, under most conditions the damage diagram differs little from the $D = 1$ curves. This lack of difference occurs because, except for shorter times and lower cyclic lives, the damage under the conditions covered by these curves is essentially all from creep. Therefore, the total amount of damage, D , approaches unity.

Also of note are the geometric configurations of the curves, particularly the flatness in the high-cycle portions of many of the curves. This flatness again occurs because the damage under these conditions is essentially all from creep. The strain level simply becomes that which corresponds to the stress to give rupture in a time of $20t_D$ and is

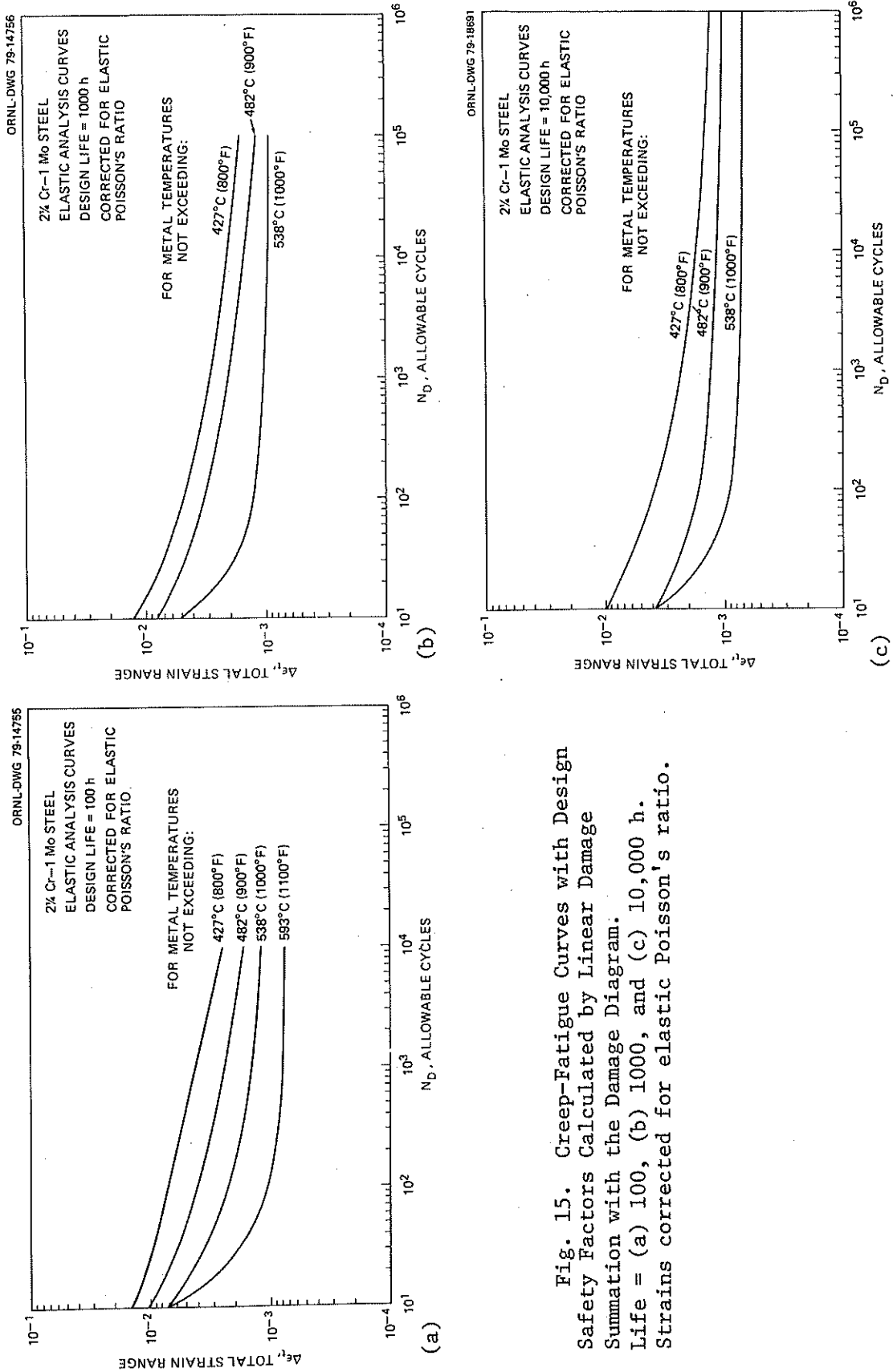


Fig. 15. Creep-Fatigue Curves with Design Safety Factors Calculated by Linear Damage Summation with the Damage Diagram. Life = (a) 100, (b) 1000, and (c) 10,000 h. Strains corrected for elastic Poisson's ratio.

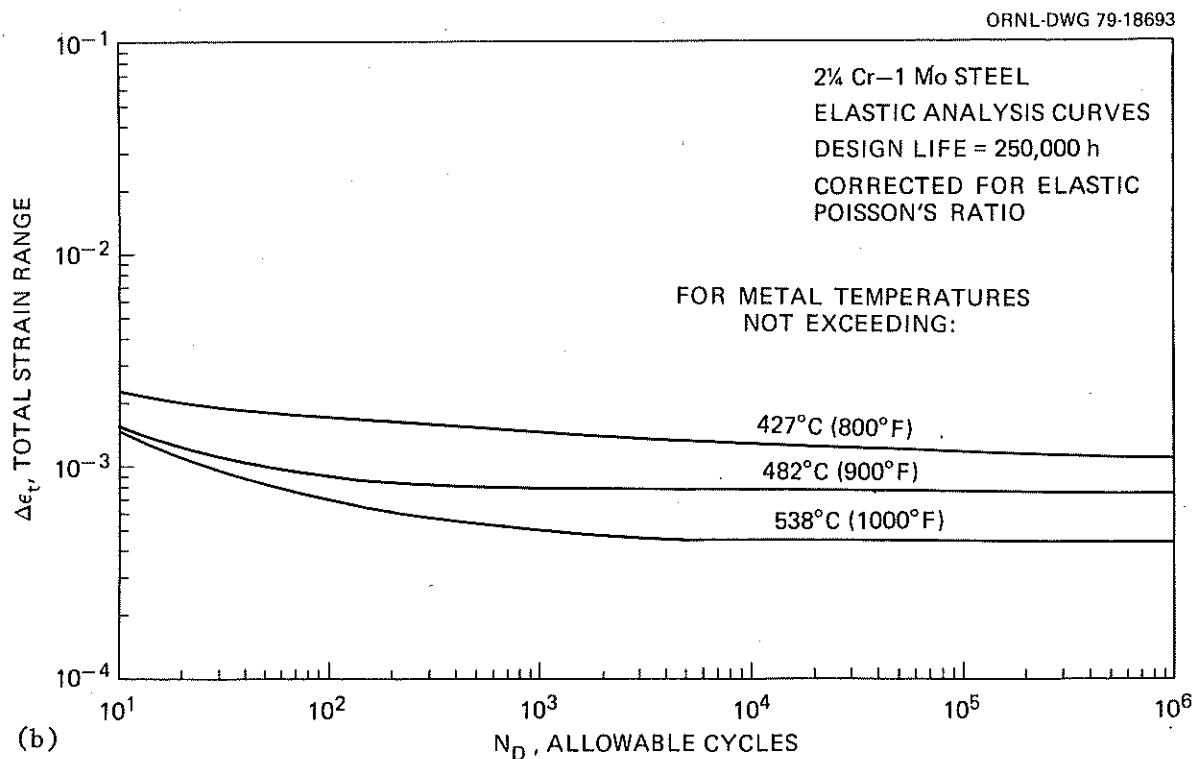
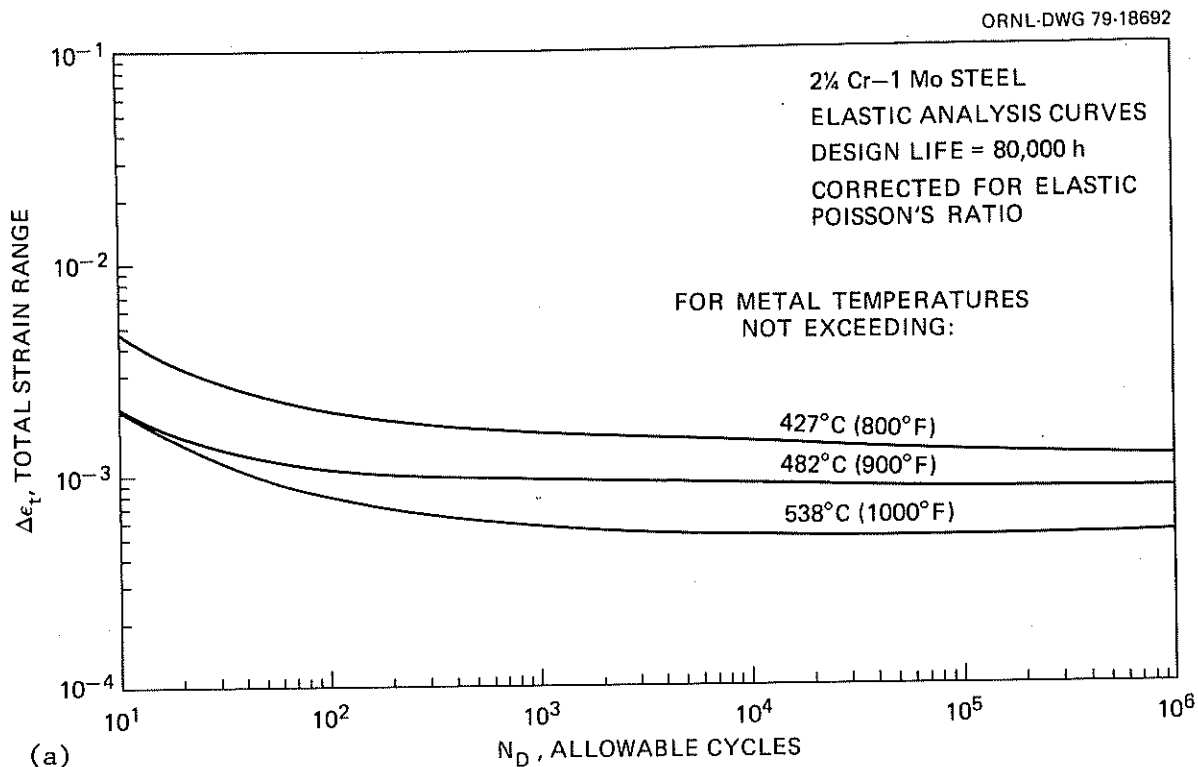


Fig. 16. Creep-Fatigue Curves with Design Safety Factors Calculated by Linear Damage Summation with the Damage Diagram. Life = (a) 80,000 and (b) 250,000 h. Strains corrected for elastic Poisson's ratio.

virtually independent of the number of cycles. Thus, the flatness directly results from the use of the linear damage summation approach in constructing the curves.

STRAIN RANGE PARTITIONING RESULTS

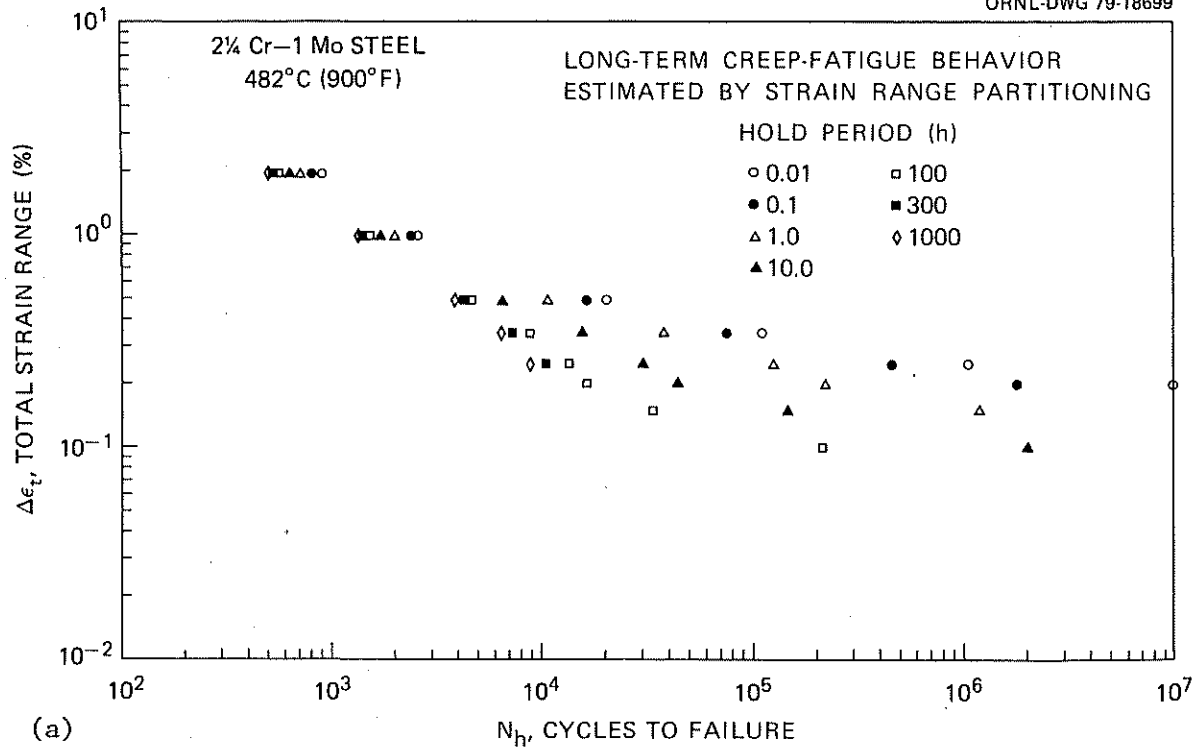
The long-term relaxation predictions were also used to estimate strain range components for use in projection of long-term creep-fatigue behavior by strain range partitioning. Note from Fig. 3 that "*op*" strain is the most damaging at high strains, while "*pc*" strain is the most damaging at low strains. For our long-term predictions, whichever of these two was most damaging was used in each particular situation. Figure 17 illustrates average long-term predictions from this method. The predicted behavior was somewhat similar to that obtained by the linear summation of damage approach, although the actual numbers change. In general the SRP predictions tend to be more optimistic at high strains but gradually approach the linear damage predictions at lower strains.

Since the SRP approach deals only with inelastic strains, uncertainties would appear to be magnified under conditions of essentially elastic behavior. To yield predictions under such conditions, we arbitrarily imposed a minimum inelastic strain range of 0.001% on all conditions, regardless of the actual predicted strains. This assumption could distort the very high cycle behavior. However, since we are interested in constructing elastic analysis curves to 10^6 cycles only, the assumption should not greatly influence the results.

Another uncertainty arises in attempting to apply design safety factors to the SRP predictions. The factors used for the linear damage predictions were obtained as current Code practice. However, there is no such practice for the SRP results. Therefore, since the SRP results are presented only for comparison, we chose to calculate average curves only and did not attempt to apply design safety factors.

In view of the comparisons with experimental data, the SRP approach may very well be more realistic than the linear summation of damage approach for this material. On the other hand, neither method directly addresses the strong environmental effects on the creep-fatigue behavior

ORNL-DWG 79-18699



ORNL-DWG 79-18700

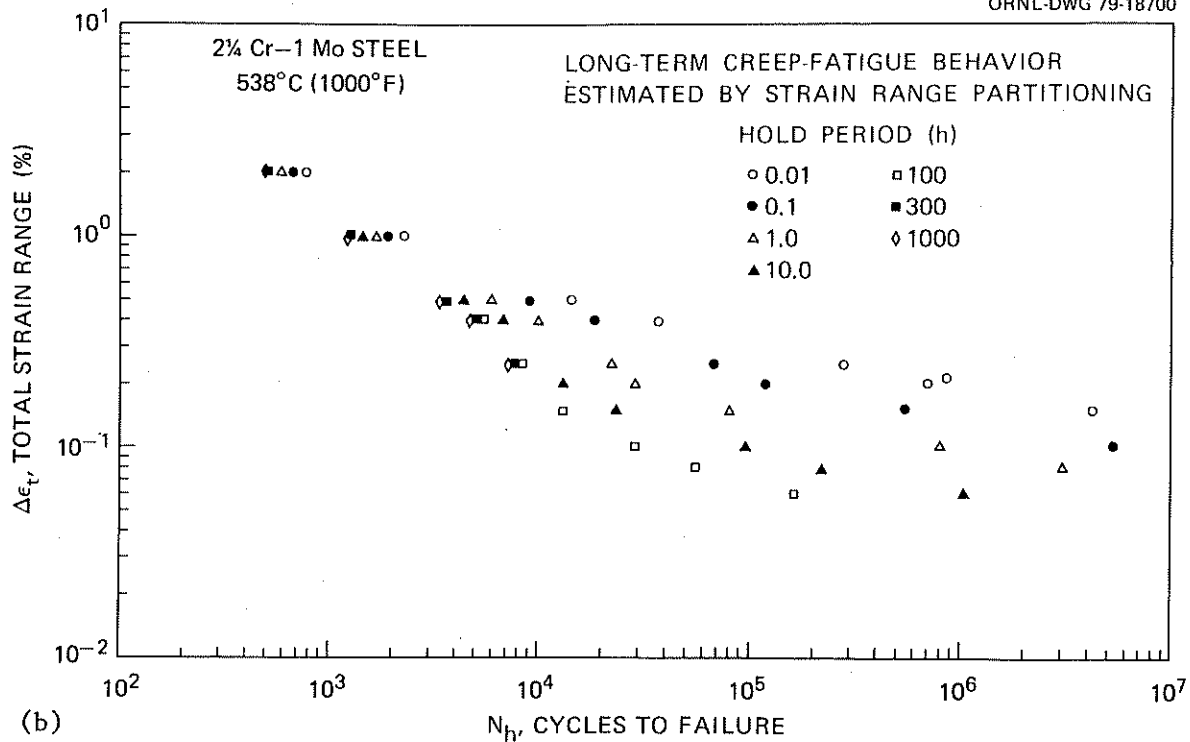


Fig. 17. Projected Average Creep-Fatigue Behavior by Strain Range Partitioning at (a) 482°C (900°F) and (b) 538°C (1000°F).

of this material. Moreover, a significant amount of work needs to be done before the true accuracy of the strain range partitioning approach for the examination of the long-term creep-fatigue behavior of 2 1/4 Cr-1 Mo steel can be determined.

DAMAGE RATE RESULTS

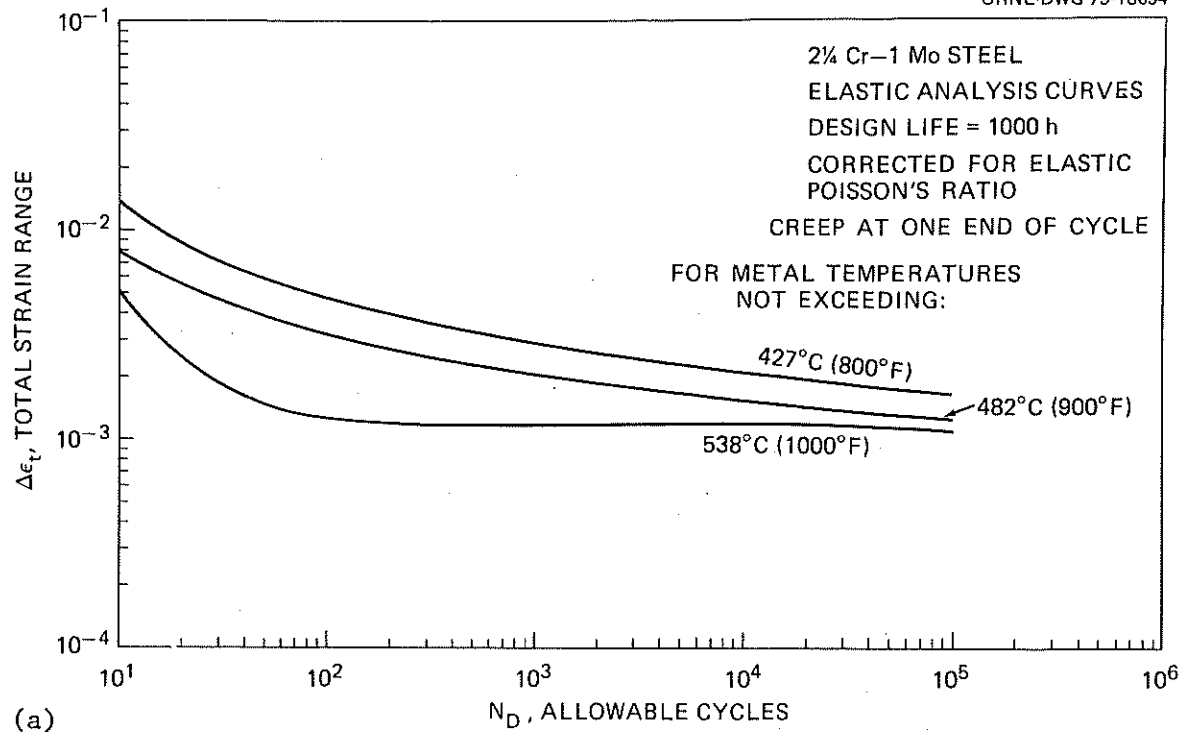
We projected no long-term behavior using the damage rate approach because our work with this method is preliminary.

STATUS

The elastic curves constructed with the linear damage summation damage diagram (Figs. 15 and 16) appear to be the optimum set of results based on current ASME Code Case N-47 rules. However, note that the hysteresis loop used in constructing these curves assumed zero mean stress. Such an assumption is adequate for this application if creep (or relaxation) can potentially occur at both ends of the loop. However, if creep can occur at only one end of the loop (e.g., if the other end is at a temperature below the creep range), a mean stress will develop in the direction of the end with no creep. In this case the stresses during relaxation or creep on the first end will be lower than those used in this report, and Figs. 15 and 17 may be overconservative. To avoid this undue conservatism the curves in Figs. 18 and 19, constructed by the Schultz method documented in the Appendix, are recommended for use when creep can occur at only one end of the cycle. (The 100-h curves were unchanged.)

The validation of alternative techniques for the prediction of long-term creep-fatigue behavior should be vigorously pursued since the linear damage approach appears to have significant potential shortcomings. Also, alternative methods for the presentation of the elastic analysis curves should be studied. The long-term constant life curves are so dominated by creep damage that they contain little information. Moreover, the curves in Figs. 15 and 16 (and the existing elastic analysis curves in Code Case N-47 for other materials) are so conservative that they may be of little general usefulness.²⁰ Alternatives that could easily be pursued might

ORNL-DWG 79-18694



ORNL-DWG 79-18696

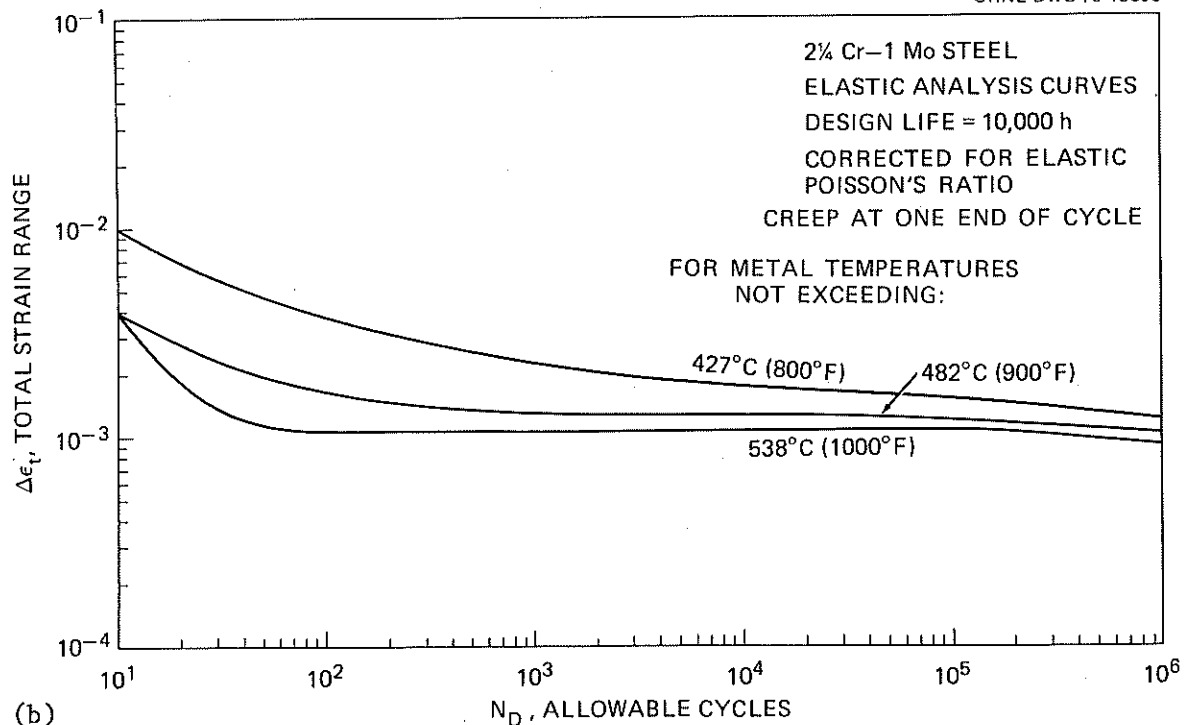


Fig. 18. Creep-Fatigue Curves with Design Safety Factors Calculated by Linear Damage Summation with the Damage Diagram, Assuming Relaxation at only one End of the Cycle. Life = (a) 1000, and (b) 10,000 h. Strains corrected for elastic Poisson's ratio.

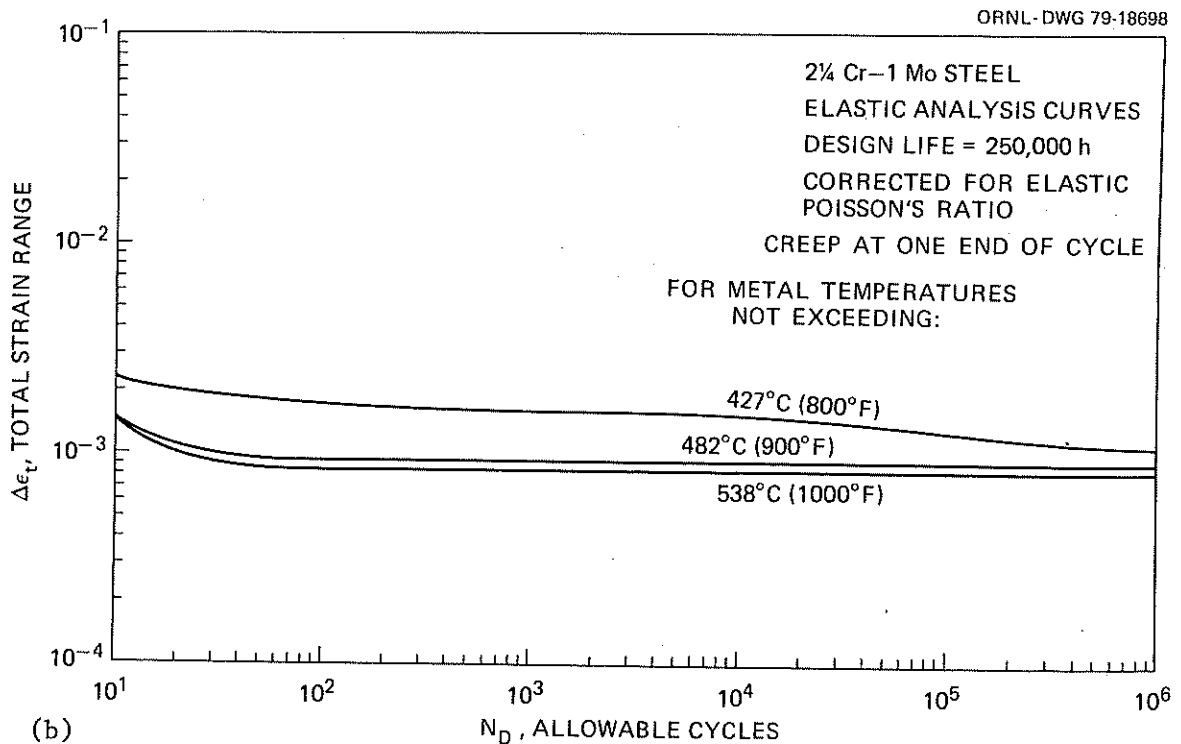
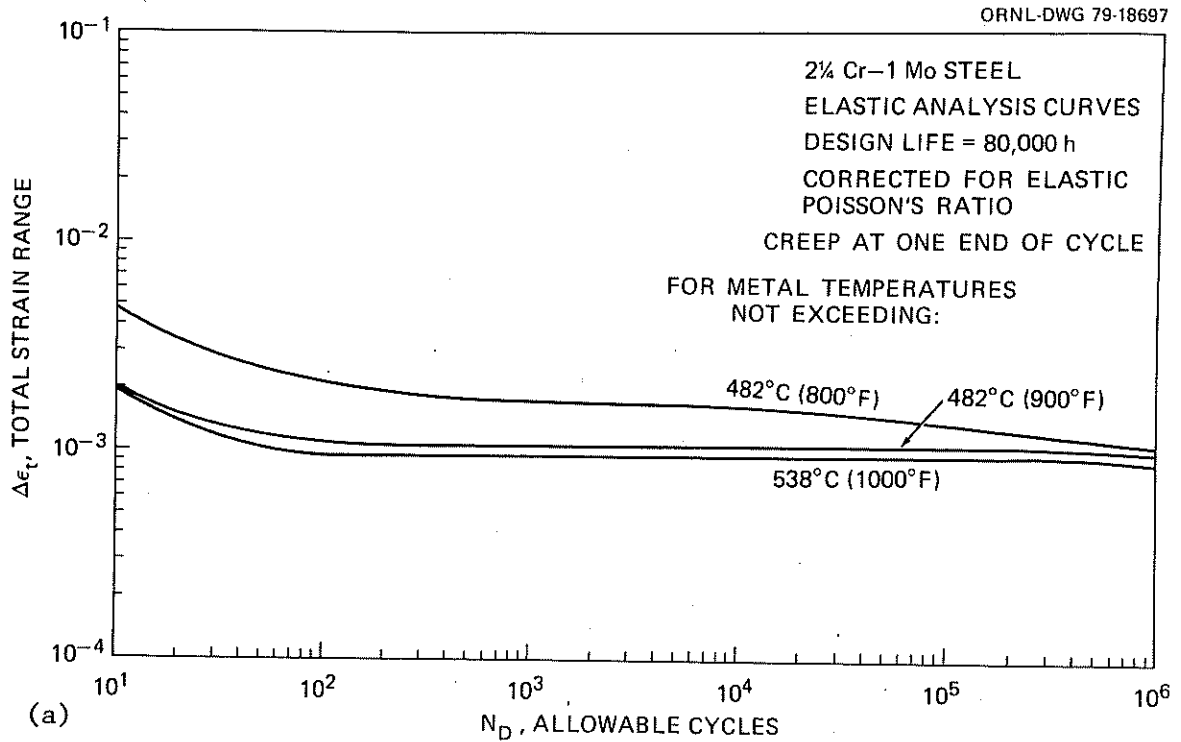


Fig. 19. Creep-Fatigue Curves with Design Safety Factors Calculated by Linear Damage Summation with the Damage Diagram, Assuming Relaxation at Only One End of the Cycle. Life = (a) 80,000 and (b) 250,000 h. Strains corrected for elastic Poisson's ratio.

include use of the constant hold-time plots (such as Fig. 11) or plots of creep damage per cycle vs hold time for various strain ranges. The ASME Working Group on Creep-Fatigue is currently pursuing such alternatives.

CONCLUSIONS

1. Available creep-fatigue for 2 1/4 Cr-1 Mo steel can be reasonably well described by the techniques of linear damage summation, strain range partitioning, and damage rate analysis. However, all methods yield large uncertainties upon extrapolation to longer times and lower strain ranges. None of the methods appear to reflect true trends in this region.

2. Available creep-fatigue data can be indirectly and artificially extrapolated to long times with any of the above techniques in conjunction with representations of cyclic stress-strain and creep behavior.

3. Using the above extrapolations we constructed elastic analysis creep-fatigue curves for this material at the request of the ASME Working Group on Creep Fatigue.

4. The resultant elastic analysis curves (and the curves for other materials currently in Code Case N-47) appear to be so conservative that they can very seldom be used. Alternative methods for the presentation of creep-fatigue behavior for elastic analysis should be pursued.

ACKNOWLEDGMENTS

The author would like to thank D. O. Hobson, J. P. Strizak, and C. R. Brinkman for reviewing the contents of this report. Thanks also go to G. M. Slaughter and J. R. DiStefano for permission to publish the results. The contributions of the members and associates of the ASME Working Group on Creep-Fatigue (chaired by R. D. Campbell) also deserve to be acknowledged. Finally, thanks go to B. G. Ashdown for editing and to A. F. Rice for preparing the final manuscript.

REFERENCES

1. L. F. Coffin, A. E. Carden, S. S. Manson, L. K. Severud, and W. L. Greenstreet, *Time-Dependent Fatigue of Structural Alloys*, ORNL-5073 (January 1977).
2. American Society of Mechanical Engineers, *Interpretations of the ASME Boiler and Pressure Vessel Code, Case N-47*, New York, 1974.
3. M. K. Booker, *Construction of Creep-Fatigue Elastic-Analysis Curves and Interim Analysis of Long-Term Creep-Fatigue Data for 2 1/4 Cr-1 Mo Steel*, ORNL/TM-6324 (July 1978).
4. S. S. Manson, "The Development and Application of Strainrange Partitioning as a Tool in the Treatment of High Temperature Metal Fatigue," pp. K-1-K-11 in *Characterization of Low Cycle High Temperature Fatigue by the Strainrange Partitioning Method*, AGARD-CP-243, North Atlantic Treaty Organization Advisory Group for Aerospace Research and Development, London, 1978.
5. S. Majumdar and P. S. Maiya, "A Damage Equation for Creep-Fatigue Interaction," pp. 323-35 in *Creep-Fatigue Interaction*, MPC-3, American Society of Mechanical Engineers, New York, 1976.
6. E. L. Robinson, "Effect of Temperature Variation on the Creep Strength of Steels," *Trans. ASME* 60: 253-59 (1938).
7. S. Taira, "Lifetime of Structures Subjected to Varying Load and Temperature," pp. 96-119 in *Creep in Structures*, N. J. Hoff, Ed., Springer Verlag, Berlin, 1962.
8. R. D. Campbell, "Creep/Fatigue Interaction Correlation for 304 Stainless Steel Subjected to Strain-Controlled Cycling with Hold Times at Peak Strain," *J. Eng. Ind.* 93: 887-92 (November 1971).
9. C. R. Brinkman, M. K. Booker, J. P. Strizak, and W. R. Corwin, "Elevated-Temperature Fatigue Behavior of 2 1/4 Cr-1 Mo Steel," *J. Pressure Vessel Technol.* 97(4): 252-57 (November 1975).

10. C. R. Brinkman, J. P. Strizak, and M. K. Booker, "Experiences in Use of Strain-Range Partitioning for Predicting Time-Dependent, Strain-Controlled Cyclic Lifetimes of Uniaxial Specimens of 2 1/4 Cr-1 Mo Steel, Type 316 Stainless Steel, and Hastelloy X," pp. 15-1-15-18 in *Characterization of Low Cycle High Temperature Fatigue by the Strainrange Partitioning Method*, AGARD-CP-243, North Atlantic Treaty Organization Advisory Group for Aerospace Research and Development, London, 1978. Also see ORNL-5396 (June 1978).
11. North Atlantic Treaty Organization Advisory Group for Aerospace Research and Development, *Characterization of Low Cycle High Temperature Fatigue by the Strainrange Partitioning Method*, AGARD-CP-243, London, 1978.
12. S. S. Manson, "The Challenge to Unify Treatment of High Temperature Fatigue — A Partisan Proposal Based on Strainrange Partitioning," pp. 744-74 in *Fatigue at Elevated Temperatures*, STP-520, American Society for Testing and Materials, Philadelphia, Pa., 1973.
13. M. H. Hirschberg and G. R. Halford, *Use of Strainrange Partitioning to Predict High-Temperature Low-Cycle Fatigue Life*, NASA TN D-8072 (January 1976).
14. M. K. Booker, J. P. Strizak, and C. R. Brinkman, "Analysis of the Continuous Cycling Fatigue Behavior of 2 1/4 Cr-1 Mo Steel," report in preparation.
15. G. R. Halford, M. H. Hirschberg, and S. S. Manson, "Temperature Effects on the Strainrange Partitioning Approach for Creep-Fatigue Analysis," pp. 658-67 in *Fatigue at Elevated Temperatures*, STP-520, American Society for Testing and Materials, Philadelphia, Pa., 1973.
16. M. K. Booker, T. L. Hebble, D. O. Hobson, and C. R. Brinkman, "Mechanical Property Correlations for 2 1/4 Cr-1 Mo Steel in Support of Nuclear Reactor Systems Design," *Int. J. Pressure Vessel Piping* 5: 181-205 (1977).
17. K. D. Challenger and A. K. Miller, "A Hypothesis Concerning Creep Fatigue Interaction in 2 1/4 Cr-1 Mo Alloy Steel," unpublished manuscript from Stanford University, Palo Alto, Calif., 1979.

18. M. K. Booker, *An Interim Analysis of the Creep Strain-Time Characteristics of Annealed and Isothermally Annealed 2 1/4 Cr-1 Mo Steel*, ORNL/TM-5831 (June 1977).
19. M. K. Booker, "Analytical Description of the Effects of Melting Practice and Heat Treatment on the Creep Properties of 2 1/4 Cr-1 Mo Steel," pp. 323-43 in *Effects of Melting and Processing Variables on the Mechanical Properties of Steel*, G. V. Smith, Ed., American Society of Mechanical Engineers, New York, 1977.
20. Private Communication, ASME Working Group on Creep-Fatigue, to M. K. Booker, Oak Ridge National Laboratory, 1978.

APPENDIX

Babcock and Wilcox letter documenting the procedure used to generate the creep damage for the high-cycle end of the elastic design fatigue curves for cycles with a hold period at only one extreme.

Babcock & Wilcox

Research and Development Division

P.O. Box 835, Alliance, Ohio 44601

Telephone: (216) 821-9110

June 1, 1979

Mr. M. K. Booker
Oak Ridge National Lab.
P. O. Box X
Oak Ridge, Tennessee 37830

Dear Keith:

The purpose of this letter is to document the procedure used to generate the creep damage for the high cycle end of the elastic design fatigue curves for cycles with a hold-period at only one extreme.

The hysteresis loops shown in Figure 1 illustrate the behavior possible at low strain ranges with a hold-period at only one extreme of the cycle. As shown in that figure, the strain range of $\Delta\epsilon$ is obtained by cycling between strain limits of zero and $+\epsilon_1$. Note that the hold-period occurs at a fixed strain of $+\epsilon_1$. The broken line represents unloading from the maximum strain for which that unloading would remain elastic (i.e., a stress range of twice the yield stress). Note that the initial stress for any cycle is equal to the final stress of the previous cycle until the stress relaxes to a value below that represented by the point labeled "a" in Figure 1. That is, relaxation to point a is monotonic and is seen to depend on the total elapsed time as opposed to the specific duration of each individual hold-period. Subsequent to relaxing to point a, all cycles will be identical such as illustrated by the path defined by the points a, 9, 10, 11, etc.

In the above example, the creep damage can, for convenience, be considered to be composed of two separate components. Specifically:

- The creep damage incurred during monotonic relaxation from point 1 to point a.
- The incremental creep damage incurred during each subsequent cycle as a result of repetitively relaxing from point a to point 9.

A very convenient (and conservative) assumption is that the stresses represented by points a and 9 are nearly identical such that this relaxation may be ignored. In so doing, one may completely ignore the hold-time duration and be concerned with only the total design life. For example, assume that the design life is DL hours and that it takes t_f hours to relax from stress S_i (point 1 of Figure 1) to stress S_a (point a of Figure 1). The first component of creep damage is then that incurred during monotonic relaxation from S_i to S_a during t_f hours. The second component of creep damage is approximated as $(DL - t_f)$ hours at a constant stress of S_a ; i.e., $(DL - t_f)/T_{Da}$, where T_{Da} represents the time-to-rupture at a stress of S_a .

The above described procedure represents the basics of the method used to generate the creep damages previously transmitted to you.

Other hysteresis loops could have been selected as the basis of the method. For example, that shown in Figure 2. In that figure, the strain range of $\Delta\epsilon$ is obtained by cycling between $\pm\Delta\epsilon/2$. It is again assumed that the hold-period is introduced on the tensile extreme. The behavior is basically the same as that shown in Figure 1. The creep damage is, however, less than that for the situation of Figure 1. To illustrate this difference, points 1 and a of Figure 1 are shown in Figure 2 as points 1' and a'. The behavior of Figure 2 was discarded primarily because it is less conservative than the behavior of Figure 1.

The situation shown in Figure 3 might also be considered as a possible basis of generating the elastic design fatigue curves. In that figure, the strain range of $\Delta\epsilon$ is obtained by cycling between zero and $+\epsilon_1$. This situation differs from that of Figure 1 in that the hold-period is introduced at zero strain. It is seen that each cycle is identical to the previous cycle throughout the life. This is true irrespective of the strain range. Point a of Figure 1 is shown in Figure 3 as point a'. It was seen in Figure 1 that the stress at the start of any hold-period, S_i (Figure 1), is equal to or greater than the stress of point a, S_a ; i.e., S_i (Figure 1) $\geq S_a$. For the situation of Figure 3, the stress at the start of each cycle is a constant, S_i (Figure 3). It can be

Babcock & Wilcox

M. K. Booker

-3-

June 1, 1979

shown that

$$S_a \text{ (Figure 1)} = S_i \text{ (Figure 3)} + \Delta\epsilon E^P$$

where E^P represents the slope of the cyclic stress-strain curve beyond the yield stress. It is then apparent that the conditions of Figure 1 are more damaging than those of Figure 3 since:

$$S_a > S_i \text{ (Figure 3)}$$

Creep damages were generated for 800, 900 and 1000F for design lives of 10^2 , 10^3 , 10^4 , 8×10^4 , and 2.5×10^5 hours. All calculations requiring the use of the average expected UTS were based on the following values:

800F	66.89 KSI
900F	62.70 KSI
1000F	55.02 KSI

All creep strain calculations were based on the NSMH creep equation using the above average UTS values. The average expected stress rupture behavior was based on the proposed NSMH equation that you provided. That is,

$$\log t_r = -13.528 + 6.5196 U/T + 23349/T - 5693.8 (\log \sigma)/T$$

where

t_r = time to rupture (hours)

U = ultimate tensile strength (MPa) at temperature

T = temperature (K)

σ = stress (MPa)

The bilinear cyclic stress-strain curves used to define the initial stresses are shown in Figures 4, 5, and 6. These curves were constructed on the basis of the 0.10 hour hold-time data provided by you. That data is represented by the open symbols in those figures. Although not apparent, the open symbol data was plotted on the basis of stress vs. strain range/2.

To fully document the details of the procedure an example is provided. The example selected is a strain range of 1.8×10^{-3} in/in at 800F. Beyond the yield stress, the equation for the line representing the bilinear cyclic stress-strain curve is:

$$\sigma = S_y \left(1 - \frac{E^P}{E}\right) + \Delta\epsilon E^P$$

Babcock & Wilcox

M. K. Booker

-4-

June 1, 1979

That equation provides the initial stress, S_i , of 32.45 KSI for the above conditions. This corresponds to point J of Figure 1. The critical relaxation stress, S_a , (point a of Figure 1) is defined by:

$$S_a = S_y \left(\frac{E^p}{E} - 1 \right) + \Delta \epsilon E$$

For the above conditions, $S_a = 21.62$ KSI.

On the basis of uniaxial relaxation calculations, with an initial stress of 32.45 KSI, it was found that the stress relaxes to 21.62 KSI in approximately 5000 hours with an accumulated creep damage of approximately 2.6×10^{-3} . A factor of safety of 20 on creep damage results in an estimated creep damage of 0.052. As previously discussed, the creep damage is, for convenience, considered to consist of two components. The damage of 0.052 represents the damage incurred during the monotonic relaxation that occurs during the first 5000 hours of the design life. Let this damage be represented as D_{c1} .

The second component of creep damage (represented as D_{c2}) is determined by assuming that the remainder of the design life is spent at a stress of S_a ; i.e., 21.62 KSI. At a stress of 21.62 KSI, the average expected time to rupture divided by the factor of safety of 20 is 140,400 hours.

For a design life of 250,000 hours:

$$D_{c2} = \frac{250,000 - 5,000}{140,400} = 1.745$$

and

$$D_{CT} = D_{c1} + D_{c2} = 0.052 + 1.745 = 1.797$$

indicating that the assumptions are too conservative for a design life of 250,000 hours. Specifically, a hold-period should be defined during which the stress could repetitively relax from S_a to some lower value after the initial 5,000 hours of the design life.

For a design life of 80,000 hours:

$$D_{c2} = \frac{80,000 - 5,000}{140,400} = 0.534$$

and

$$D_{CT} = D_{c1} + D_{c2} = 0.052 + 0.534 = 0.586$$

Babcock & Wilcox

M. K. Booker

-5-

June 1, 1979

Using the bilinear damage interaction diagram (0.1, 0.1) the allowable fatigue damage, D_f , is 0.046.

For a design life of 10,000 hours:

$$D_{c2} = \frac{10,000 - 5,000}{140,400} = 0.036$$

and

$$D_{cT} = 0.052 + 0.036 = 0.088$$

The allowable fatigue damage, D_f , is then 0.208.

For a design life of 1,000 hours the procedure is changed since monotonic relaxation to S_a requires a time in excess of the design life. In this case, D_{c1} is determined by allowing 1,000 hours of relaxation from an initial stress of 32.45 KSI. With the factor of safety of 20, this damage is determined to be 0.019. Note that D_{c2} is zero, so that the total creep damage, D_{cT} , is 0.019. The allowable fatigue damage, D_f , is then 0.829.

All of the previously transmitted results are provided in Table 1. The design allowable number of cycles is obtained by multiplying the corresponding allowable cycles from the continuous cycling design fatigue curve by D_f as provided in Table 1.

At higher strain ranges this method will provide results that are more conservative than those obtained using the standard method previously accepted by the WGCF. This additional conservatism is due to the simplifying assumption that relaxation does not progress below S_a . At those strain ranges for which results are available for both methods, it is quite correct to accept the least conservative solution. Similarly, at strain ranges for which solutions were not obtained by either method, it is considered acceptable to interpolate or fair-in the missing data.

As you recently pointed out, the present method can, in some cases, result in predictions that are more conservative than the standard method even at the lower strain ranges. This additional conservatism is the result of assuming that the strain range $\Delta\epsilon$ is obtained by cycling between zero and ϵ_1 as opposed to cycling between $\pm\Delta\epsilon/2$. As a result of this assumption, the initial

Babcock & Wilcox
M. K. Booker

-6-

June 1, 1979

stress is increased by a factor of at least 2. At the higher strain ranges, the cycle definition (such as shown in Figures 1, 2, and 3) does not affect the results; thus any choice is acceptable. However, as previously discussed, the cycle defined in Figure 1 appears to be the most acceptable choice at the lower strain ranges.

A final consideration worth mentioning is the use of the 0.1 hour hold-time data to generate the cyclic stress-strain curves. It is obvious that the hold-time must increase as the allowable cycles decrease for a fixed design life. For consistency, a multitude of cyclic stress-strain curves should have been used. At this time, I don't think the additional effort is justified.

It is hoped that this exercise is of value in your effort to construct the elastic design fatigue curves. Perhaps it will also serve to focus attention on some of the short-comings of the basic concept of elastic design fatigue curves.

I do want to thank you for the considerable and prompt help that you have provided. I look forward to seeing you in New York.

Yours truly,

THE BABCOCK & WILCOX COMPANY
Alliance Research Center

C. C. Schultz
C. C. Schultz
Applied Mechanics

mad

Attachments

cc: R. D. Campbell
J. M. Duke
B. M. Hinton - NED
L. K. Severud
J. M. Tanzosh - NED
W. Veljovich

TABLE 1. ALLOWABLE FATIGUE DAMAGE FOR
VARIOUS DESIGN LIVES

800F

$\Delta\epsilon$ ($\times 10^3$ in/in)	2.5×10^5 hrs	8×10^4 hrs	10^4 hrs	10^3 hrs	10^2 hrs
1.0	0.097	0.118	0.694	0.937	0.982
1.1	0.093	0.097	0.541	0.901	0.973
1.2	0.091	0.095	0.442	0.874	0.964
1.3	0.090	0.094	0.415	0.874	0.964
1.4	0.089	0.094	0.388	0.865	0.955
1.5	0.088	0.093	0.361	0.856	0.955
1.6	0.078	0.092	0.325	0.847	0.955
1.7	0.035	0.083	0.289	0.838	0.946
1.8		0.046	0.208	0.829	0.946
1.9			0.091	0.793	0.946
2.0			0.065	0.604	0.937
2.1			0.014	0.208	0.910
2.2				0.092	0.838

900F

$\Delta\epsilon$ ($\times 10^3$ in/in)	2.5×10^5 hrs	8×10^4 hrs	10^4 hrs	10^3 hrs	10^2 hrs
0.8	0.253	0.262	0.316	0.748	0.946
0.9	0.099	0.099	0.099	0.595	0.910
1.0	0.096	0.097	0.098	0.550	0.892
1.1	0.079	0.092	0.097	0.505	0.883
1.2		0.066	0.096	0.469	0.874
1.3			0.088	0.424	0.856
1.4			0.049	0.298	0.847
1.5				0.094	0.820
1.6				0.070	0.649
1.7				0.018	0.244

1000F

$\Delta\epsilon$ ($\times 10^3$ in/in)	2.5×10^5 hrs	8×10^4 hrs	10^4 hrs	10^3 hrs	10^2 hrs
0.6	0.721	0.748	0.775	0.802	0.901
0.7	0.595	0.622	0.658	0.694	0.829
0.8	0.460	0.487	0.532	0.577	0.739
0.9	0.316	0.343	0.388	0.442	0.631
1.0	0.094	0.100	0.262	0.325	0.523
1.1		0.060	0.097	0.298	0.496
1.2			0.063	0.109	0.478
1.3				0.087	0.451
1.4				0.038	0.226
1.5					0.089

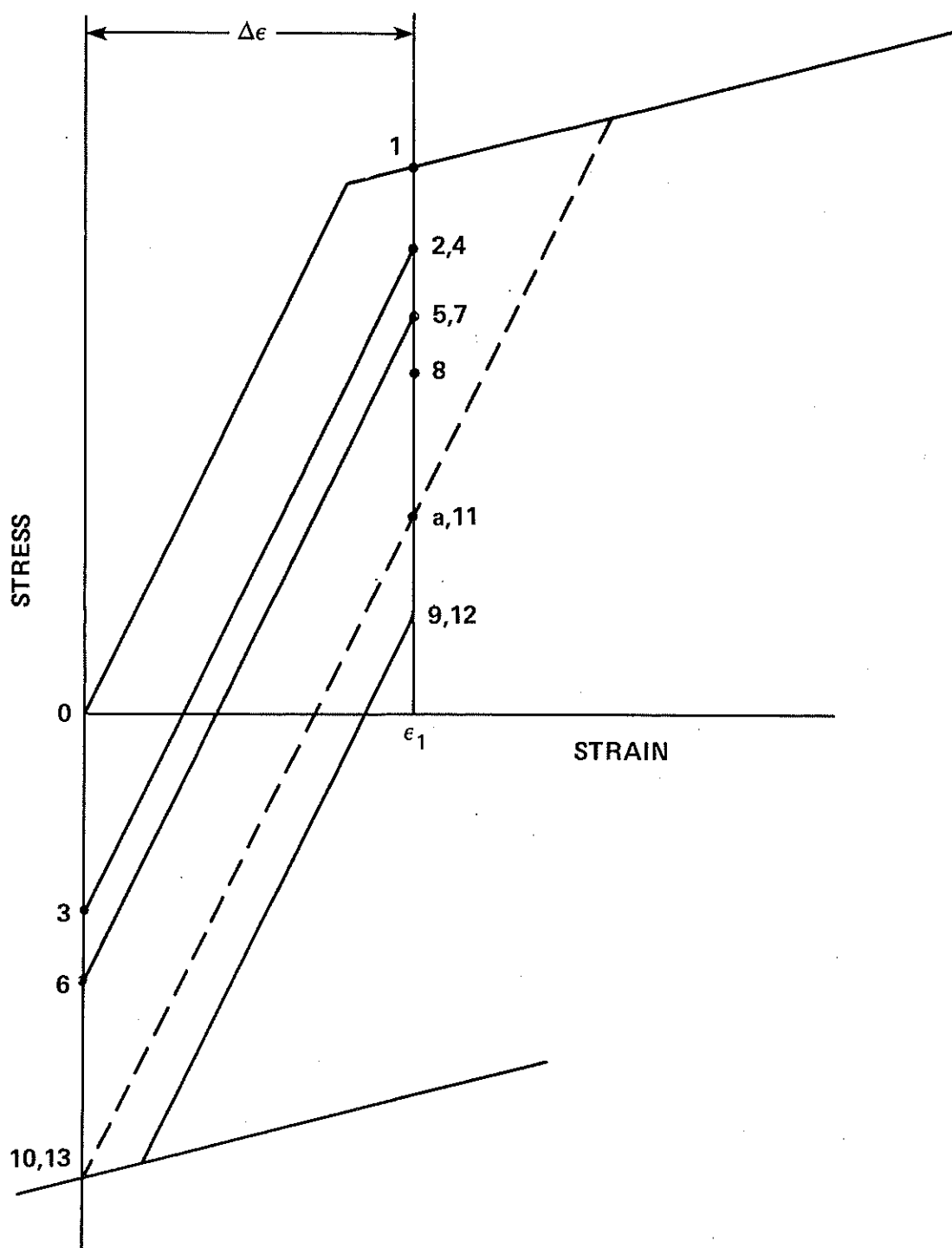


Fig. 1.

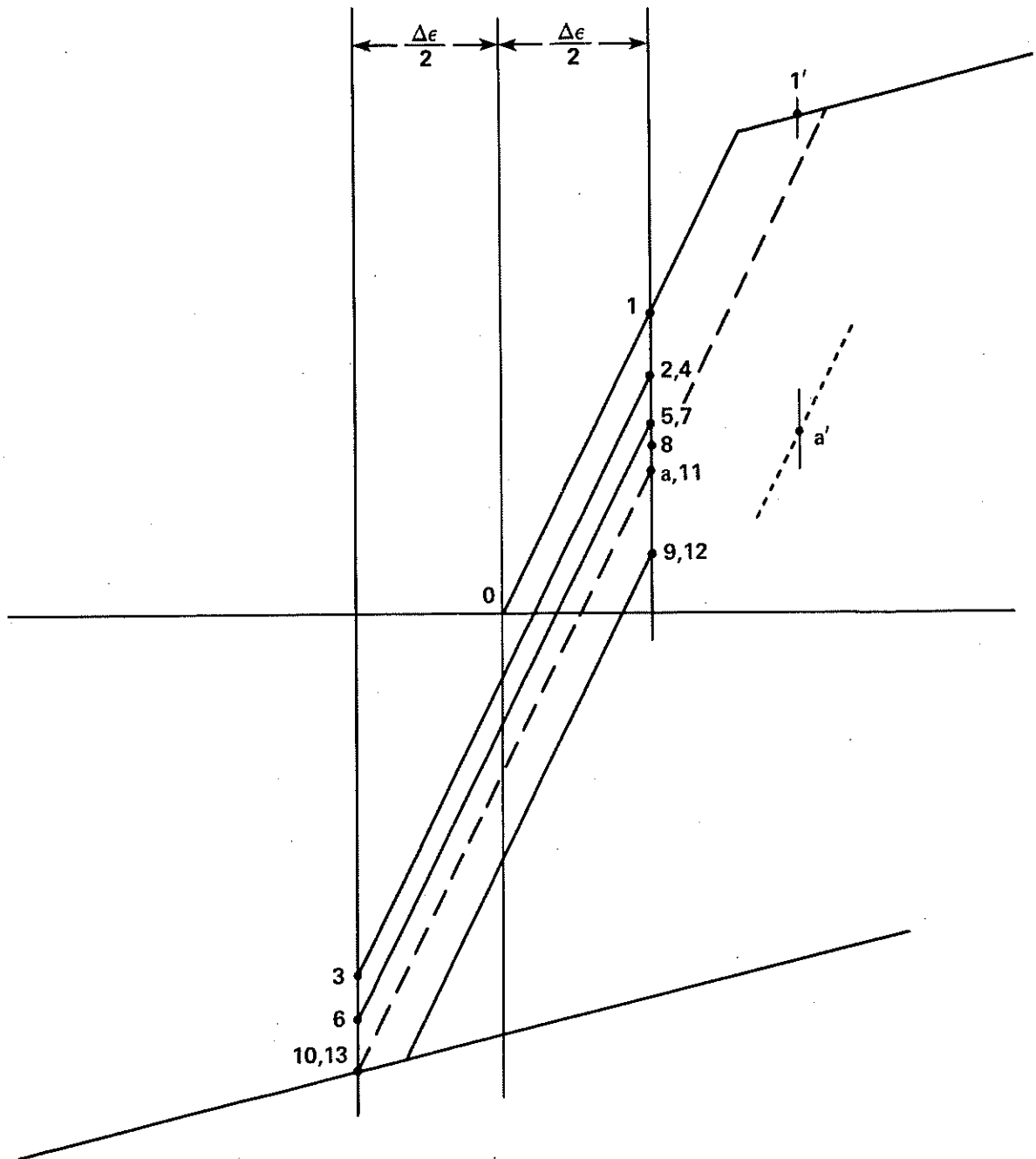


Fig. 2.

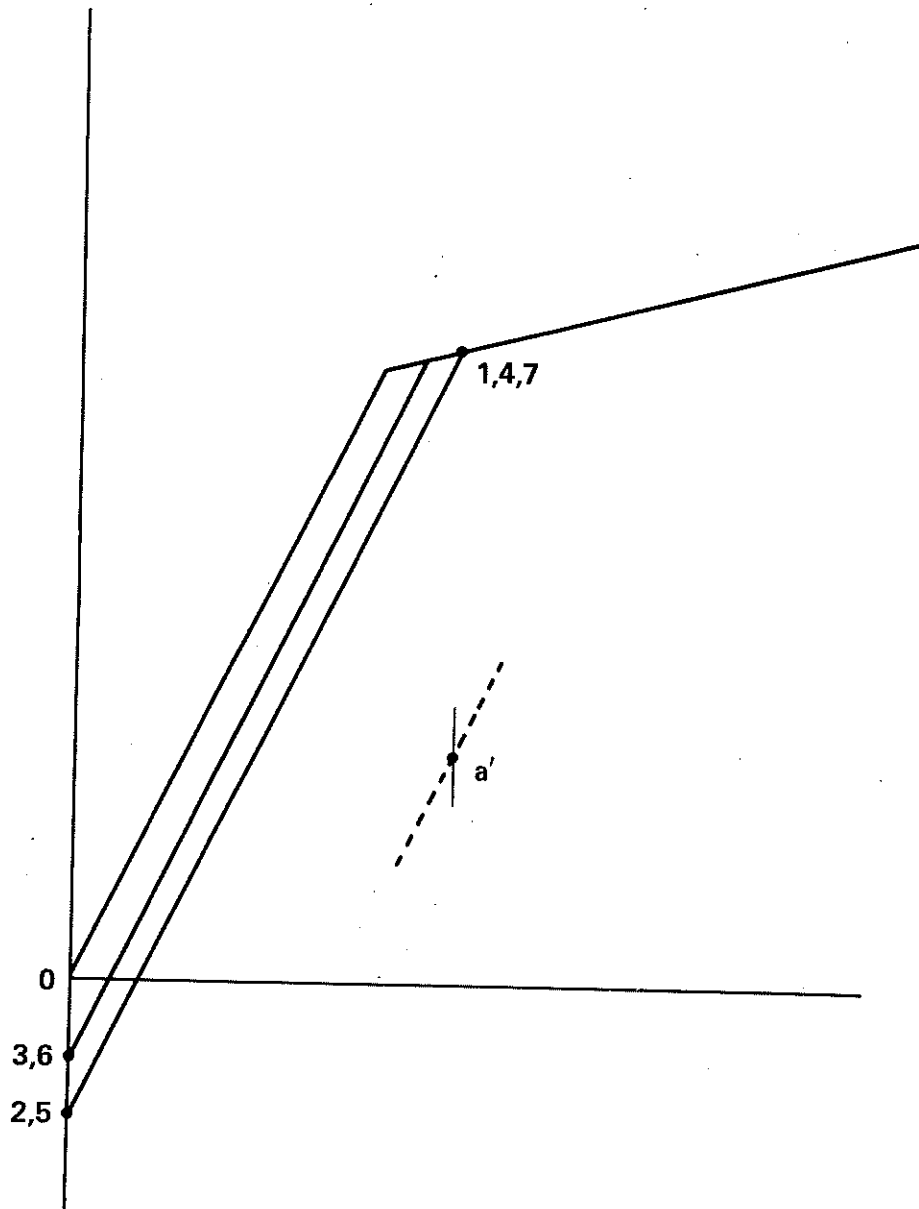


Fig. 3.

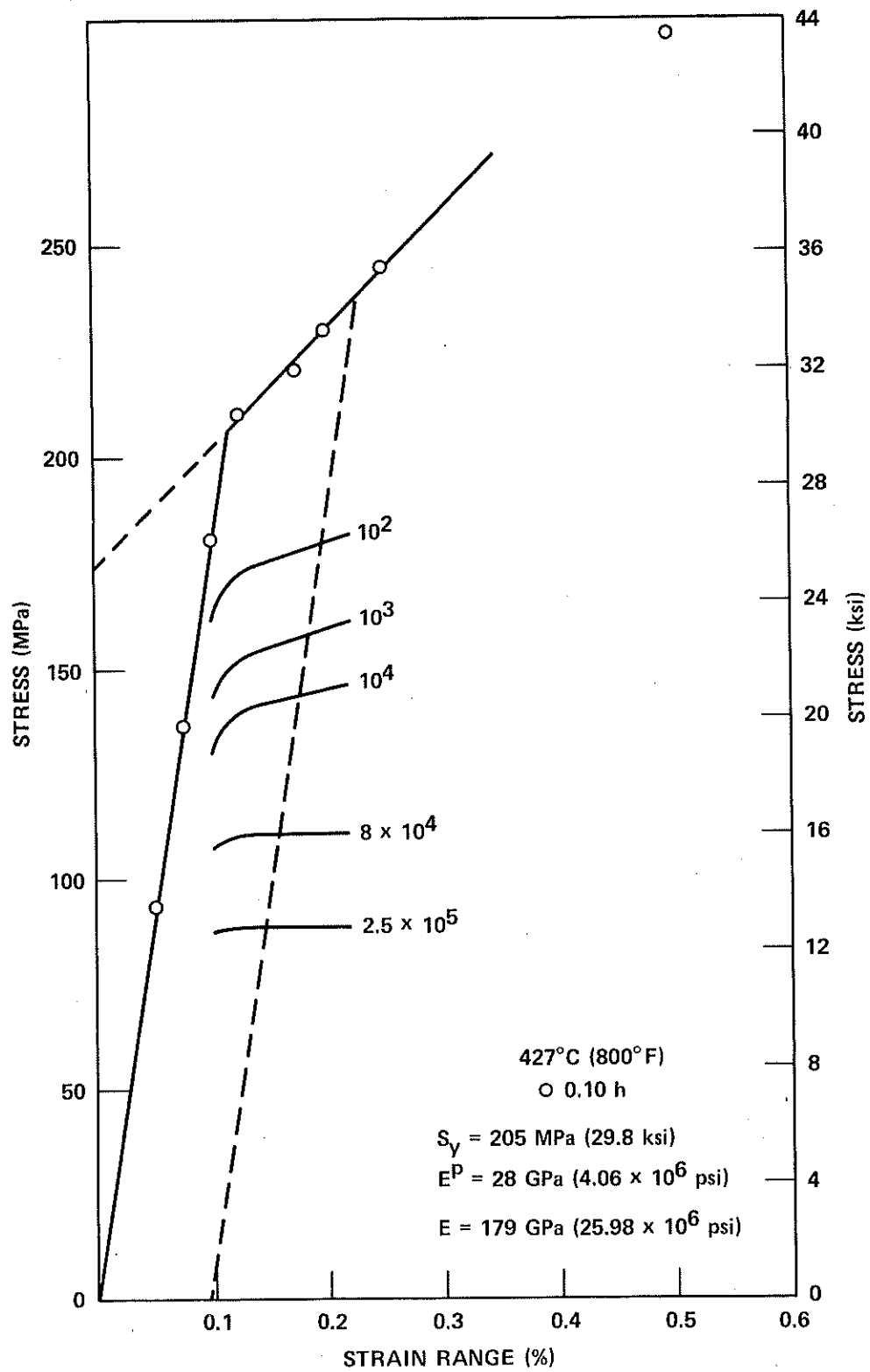


Fig. 4.

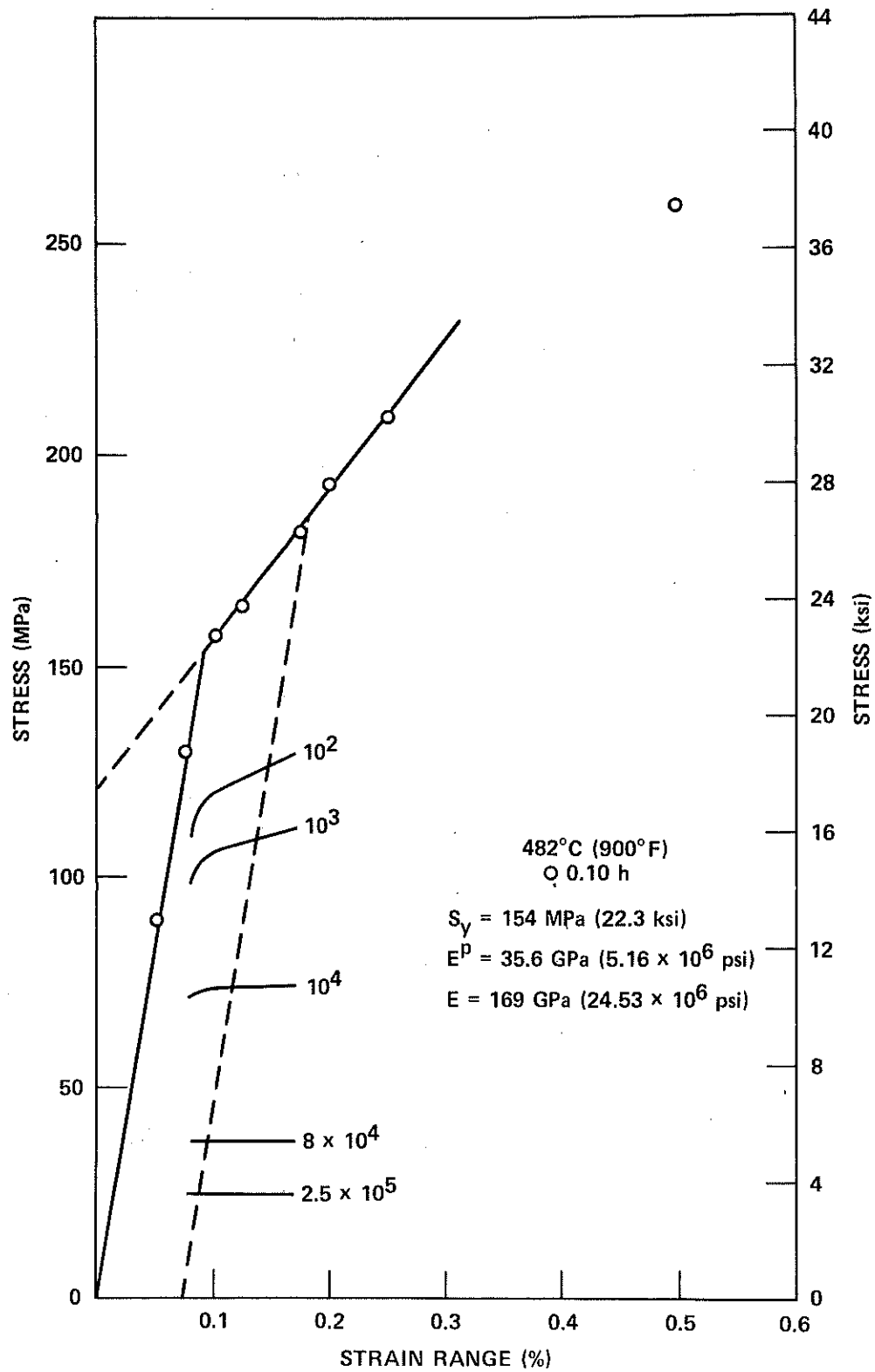


Fig. 5.

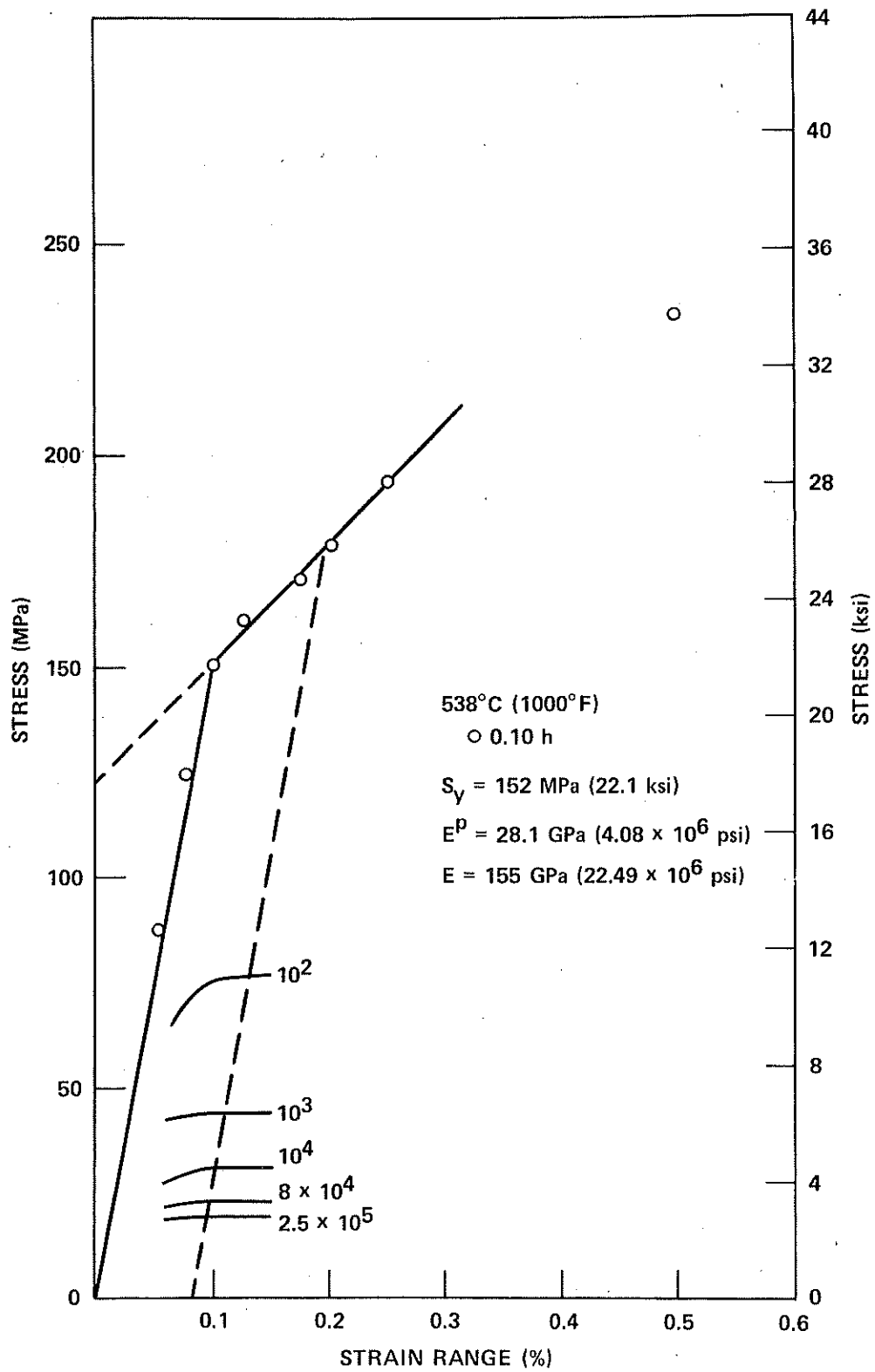


Fig. 6.